


12-2014

Atom-Based Geometrical Fingerprinting of Conformal Two-Dimensional Materials

Mehrshad Mehboudi

University of Arkansas, Fayetteville

Follow this and additional works at: <http://scholarworks.uark.edu/etd>

 Part of the [Atomic, Molecular and Optical Physics Commons](#), [Biophysics Commons](#), [Engineering Physics Commons](#), and the [Structural Materials Commons](#)

Recommended Citation

Meboudi, Mehrshad, "Atom-Based Geometrical Fingerprinting of Conformal Two-Dimensional Materials" (2014). *Theses and Dissertations*. 2031.

<http://scholarworks.uark.edu/etd/2031>

This Thesis is brought to you for free and open access by ScholarWorks@UARK. It has been accepted for inclusion in Theses and Dissertations by an authorized administrator of ScholarWorks@UARK. For more information, please contact scholar@uark.edu, ccmiddle@uark.edu.

Atom-Based Geometrical Fingerprinting
of Conformal Two-Dimensional Materials

Atom-Based Geometrical Fingerprinting of Conformal Two-Dimensional Materials

A thesis submitted in partial fulfillment
of the requirements for the degree of
Master of Science in Microelectronics-Photonics

by

Mehrshad Mehboudi
University of Tehran
Bachelor of Science in Mechanical Engineering, 2004
Iran University of Science and Technology
Master of Science in Mechanical Engineering, 2007

December 2014
University of Arkansas

This thesis is approved for recommendation to the Graduate Council.

Dr. Salvador Barraza Lopez
Thesis Director

Dr. Douglas Spearot
Committee Member

Dr. Huaxiang Fu
Committee Member

Prof. Ken Vickers
Ex-officio Member

The following signatories attest that all software used in this thesis was legally licensed for use by Mehrshad Mehboudi for research purposes and publication.

Mr. Mehrshad Mehboudi, Student

Dr. Salvador Barraza-Lopez, Thesis Director

This thesis was submitted to <http://www.turnitin.com> for plagiarism review by the TurnItIn company's software. The signatories have examined the report on this thesis that was returned by TurnItIn and attest that, in their opinion, the items highlighted by the software are incidental to common usage and are not plagiarized material.

Dr. Rick Wise, Program Director

Dr. Salvador Barraza-Lopez, Thesis Director

Abstract

The shape of two-dimensional materials plays a significant role on their chemical and physical properties. Two-dimensional materials are basic meshes that are formed by mesh points (vertices) given by atomic positions, and connecting lines (edges) between points given by chemical bonds. Therefore the study of local shape and geometry of two-dimensional materials is a fundamental prerequisite to investigate physical and chemical properties. Hereby the use of discrete geometry to discuss the shape of two-dimensional materials is initiated.

The local geometry of a surface embodied in 3D space is determined using four invariant numbers from the metric and curvature tensors which indicates how much the surface is stretched and curved under a deformation as compared to a reference pre-deformed conformation.

Many different disciplines advance theories on conformal two-dimensional materials by relying on continuum mechanics and fitting continuum surfaces to the shape of conformal two-dimensional materials. However two-dimensional materials are inherently discrete. The continuum models are only applicable when the size of two-dimensional materials is significantly large and the deformation is less than a few percent. In this research, the knowledge of discrete differential geometry was used to tell the local shape of conformal two-dimensional materials. Three kind of two-dimensional materials are discussed: 1) one atom thickness structures such as graphene and hexagonal boron nitride; 2) high and low buckled 2D meshes like stanene, leadene, aluminum phosphate; and, 3) multi layer 2D materials such as Bi_2Se_3 and WSe_2 . The lattice structures of these materials were created by designing a mechanical model - the mechanical model was devised in the form of a Gaussian bump and density-functional theory was used to inform the local height; and, the local geometries are also discussed.

تو کی بکام دل به لب لعل اوریم
در خون دل نشسته چو یاقوت احمریم
چون صوفیان به حالت وجدند و در سماع
مانندیم به سبده دستی بر آوریم

Acknowledgements

Foremost, I would like to express my special thanks to my thesis director Prof. Salvador Barraza-Lopez for his patience and continuous support toward completion of this thesis.

My sincere thanks to Prof. Ken Vickers, and Dr. Rick Wise, the directors of the microEP program for all their help, guidance, motivation, enthusiasm, and immense patronage.

I would like to thank the rest of my group members and collaborators, especially Dr. Alejandro Pacheco for his description of structures with defects, Dr. Edmund Harris for discussions, Dr. Humberto Terrones for providing geometries, and Dr. Pablo Rivero for all his help and consulting.

I would like to thank my wife and my son for helping me and loving me during completing my research.

This program is financially supported by the Arkansas Biosciences Institute, and the Award TG: PHY090002. Any opinions, findings, and conclusions or recommendations expressed in this Material are those of the author and do not necessarily reflect the views of the National Science Foundation.

This work was supported in part by the National Science Foundation under grants MRI #0722625, MRI-R2 #0959124, and #0918970.

- Star of Arkansas - MRI #0722625
- CI-TRAIN - #0918970
- Razor - MRI-R2 #0959124

Dedication

This thesis is dedicated to my family and my research group. I hope it can help for better understanding of the properties of two-dimensional materials.

Table of Contents

Chapter 1:	Introduction.....	1
Chapter 2:	2D Materials History and Impact.....	3
2.1	Lattice Structure of Graphene	3
2.2	Electronic Properties of Graphene and other Dirac Materials	4
2.3	Other 2D Materials.....	5
2.4	Properties of 2D Materials	6
Chapter 3:	Geometry of 2D Materials	7
3.1	Deformation in 2D Materials	7
3.2	Lack of Accuracy of Continuum Mechanics for 2D Materials:.....	8
3.3	Discrete Geometry Framework	9
3.3.1	Differential Geometry Concepts.....	10
3.3.2	Discrete Differential Geometry Concepts:.....	17
3.4	Metric Computation for Different Lattices	23
Chapter 4:	Discrete Curvature and Metric Calculation for Various Lattices	25
Chapter 5:	Building Structural Models.....	27
5.1	Hexagonal Boron-Nitride.....	28
5.2	Low-Buckled Silicene.....	30
5.3	Aluminum Phosphate	31
5.4	Bismuth Selenide.....	32
5.5	Lead.....	35
5.6	Tungsten Diselenide.....	36
5.7	Phosphorene	38
Chapter 6:	Results and Discussion	41

6.1	Curvature Computation Results for Different Lattices	41
6.2	Metric Results for Various Lattices	47
6.3	Conclusion.....	48
References		50
Appendix B: Executive Summary of Newly Created Intellectual Property		56
Appendix C: Potential Patent and Commercialization Aspects of listed Intellectual Property		
Items	57
C.1	Patentability of Intellectual Property (Could Each Item be Patented).....	57
C.2	Commercialization Prospects (Should Each Item Be Patented).....	57
C.3	Possible Prior Disclosure of IP	57
Appendix D: Broader Impact of Research.....		58
D.1	Applicability of Research Methods to Other Problems.....	58
D.2	Impact of Research Results on U.S. and Global Society	58
D.3	Impact of Research Results on the Environment.	58
Appendix E: Microsoft Project for MS MicroEP Degree Plan.....		59
Appendix F: Identification of All Software Used in Research and Thesis Generation		60
Appendix G: All Publications Published, Submitted and Planned		61

Figure 1. Graphene structure and unit cell.....	4
Figure 2. Osculating circle and tangent line.	10
Figure 3. Different osculating circles tangent to a saddle surface in one point.	11
Figure 4. Analytical Gaussian curvature of a Gaussian bump.....	14
Figure 5. The Analytical mean curvature for a Gaussian bump.	14
Figure 6. Surface with (a) positive, (b) negative and (c) zero Gaussian curvature.....	15
Figure 7. Geodesic curve on different surfaces.	16
Figure 8. Buckyball; the sum of all internal angles of a pentagon.	17
Figure 9. Veronoi tessellation for an effective surface in Gauss-Bonnet theory.	18
Figure 10. Edges and angles that are needed to find discrete curvature.	19
Figure 11. Atoms required to calculate Gaussian and mean curvature for hexagonal lattices.	20
Figure 12. Atoms required curvature for a square lattice.	26
Figure 13. Required atoms for calculating curvature in presence of defects.....	26
Figure 14. Hexagonal boron nitride lattice.	28
Figure 15. Gaussian deformation applied to hexagonal boron nitride.....	29
Figure 16. Low buckled silicene structure from various views.....	30
Figure 17. AIP with buckled square lattice is shown from different views.....	32
Figure 18. Bi_2Se_3 a 2D material with five atomic layers is shown from three views.....	33
Figure 19. Gaussian deformation applied to Bi_2Se_3 . Different colors show different layers	34
Figure 20. Optimum Height reduction in a patch of Bi_2Se_3 in different layers	35
Figure 21. Leadene a 2D material with two atomic layers is shown from three views.....	36
Figure 22. tungstan diselenide shown from three views.	37

Figure 23. phosphorene from different views	40
Figure 24. The Gaussian and mean curvature for bismuth selenide..	42
Figure 25. The Gaussian and mean curvature for tungsten diselenide..	43
Figure 26. The Gaussian and mean curvature for hexagonal boron nitride.....	44
Figure 27. The Gaussian and mean curvature for silicene.....	45
Figure 28. The Gaussian and mean curvature for high buckled stanene..	46
Figure 29. Determinant of the metric tensor, trace of metric tensor for hexagonal boron nitride	47
Figure 30. Determinant of the metric tensor, trace of metric tensor for hexagonal Bi_2Se_3	47

List of Tables:

Table 1.	Thickness results from VASP for AlP	31
Table 2.	Thickness results from VASP for Bi ₂ Se ₃	34
Table 3.	Thickness for Lead after an isotropic elongation.....	36
Table 4.	Thickness results from structural relaxation of WSe ₂	37
Table 5.	Thickness for isotropic increase in lattice constant.....	39

Introduction

Imagine one can read the newspaper headlines on a cup at breakfast time, watch a TV screen installed on the wall which has thickness less than that of paper, use a cell phone less than a millimeter thick and much faster compared to current cell phones. These are only potential electronic applications of a recently discovered class of materials that are one atom thick. The new materials may change these ideas to reality one day. Graphene, a one atom thick sheet of carbon, is the most famous 2D material [1]. Being relatively transparent to light and possessing a high electric conductivity [2], graphene can be used in conjunction with other materials to make solar voltaic panels. Such extremely thin and flexible solar voltaic panels can cover the walls of a building, the surface of a car, or surface of light post to create homemade or civic solar energy. Touch-screen electronic devices such as cell phones are another application. Instead of glass, graphene can be deposited on layers of plastic. One can expect to have flexible touch screen cell phones in the near future. Since graphene's mechanical strength is almost one hundred times higher than steel's, the device will be nearly unbreakable. In addition, carbon is naturally abundant which paves the way for production of graphene-based devices with low cost.

Graphene's high resistance to salty ionic body solutions can be added to its extraordinary flexibility and strength features, which allures biomedical scientists to use on implants in body tissues. High electric conductivity of graphene allows it to be added to the neurons which are cells in charge of transferring signals to muscles and brain. Imagine a transistor made of graphene implanted to transfer signals through damaged parts of spinal cord to undamaged parts. This application would allow disabled persons to recover their health and be able to use their damaged organ. But there are more 2D materials beyond graphene with unique properties too. Induced mechanical strain on 2D materials can change their electronic and mechanical properties

significantly. Therefore, the study of mechanical strain and deformation of 2D materials in general is a promising step towards a new generation of opto-electronic devices.

Most 2D materials have unique properties that depend on their shape. These changes in shape can be induced by a mechanical deformation or any other change in the lattice structure, such as atomistic defects. Therefore, the shape of 2D materials is an important feature which should be investigated in detail. In this research a new model for characterizing the shape of 2D materials is built. Shape, or geometry, is usually thought of to occur within a continuum but given that 2D materials are made of (discrete) atoms and atomistic bonds connecting atoms together, it is not accurate to fit any continuum model to their shape [2]. Fortunately, a mathematical tool known as discrete differential geometry is already known and it can be applied to tell the shape of 2D materials [3, 4], as it is shown for the first time in this Master's thesis.

2D Materials History and Impact

Graphene was the first 2D material exfoliated in 2004 [5]. However, long before that there were different theories and efforts to investigate the possibility of their existence. Work on graphene can be traced to the 19th century during which many chemists were working on graphene oxide [6]. The German chemist, Schafhaeuti [7, 8], added alkali metals between the layers of graphite and then exfoliated graphite using different acids such as nitric and sulfuric acids [6]. This effort was historically important because the layers of graphite retain their structure, but the distance between layers is increased. In 1968, Mermin supported the ideas of Peierls and Landau [9] made thirty years before and presented his theory expressing the idea that it is not possible to have stable 2D crystalline materials [10]. In 1986, Boehm suggested to use the term of graphene for a 2D crystalline made of carbon as a building block of graphite [11]. Finally, in 2004 Novoselov and coworkers exfoliated graphite mechanically [5]. In the ensuing 10 years, other 2D crystals were synthesized and investigated [12]. The ideas of this thesis are introduced with the use of grapheme.

1.1 Lattice Structure of Graphene

Graphene is a single atomic layer of carbon with a hexagonal lattice. The unit cell of graphene consists of two atoms (A and B) and has a diamond shape which is shown in Figure 1. This unit cell is duplicated along the two lattice vectors in creating an unextended 2D crystal. The lattice constant a is equal to equal to 0.246 nm, and the unit vectors of this hexagonal lattice are:

$$\mathbf{a}_1 = \left(\frac{\sqrt{3}}{2}, \frac{1}{2}, 0 \right) \times a \quad , \quad \mathbf{a}_2 = \left(\frac{\sqrt{3}}{2}, -\frac{1}{2}, 0 \right) \times a. \quad (\text{Equation 1})$$

Graphene has a reciprocal lattice constant equal to $\frac{4\pi}{\sqrt{3}}a$. The reciprocal lattice vectors are calculated as a function of the primitive lattice vectors satisfying

$$a_i \cdot b_j = 2\pi\delta_{ij} \quad (i, j = 1, 2). \quad (\text{Equation 2})$$

The reciprocal lattice vectors thus are:

$$b_1 = \left(\frac{2\sqrt{3}\pi}{3a}, \frac{2\pi}{a}, 0 \right), \quad b_2 = \left(\frac{2\sqrt{3}\pi}{3a}, -\frac{2\pi}{a}, 0 \right). \quad (\text{Equation 3})$$

Figure 1 shows the graphene structure and the lattice vectors.

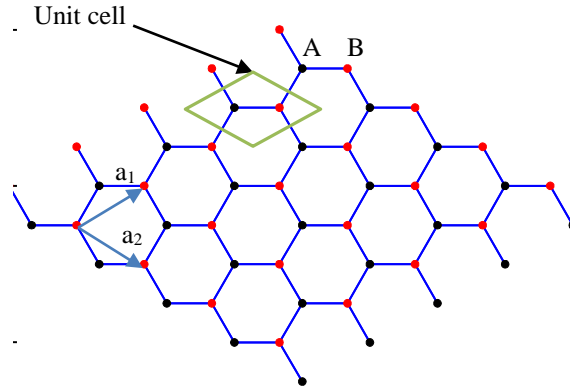


Figure 1. Graphene structure and unit cell.

1.2 Electronic Properties of Graphene and other Dirac Materials

Dirac equation is mainly used to predict the behavior of fundamental particles such as quarks and neutrinos [13]. However, recently it is also used to describe some materials known as Dirac materials [14]. Dirac materials have a cone-shaped band structure at low energy (~ 0.2 eV) around the Fermi energy induced by the symmetries of π -electrons on the hexagonal lattice. The free electrons in metals behave like massive particles and obey Schrodinger equation ($E \propto k^2$, where E

is energy and k is crystal momentum) and their energy versus momentum is a quadratic equation. In contrast, Dirac electrons have a linear dependency of energy on momentum and they behave like massless fermions $E \propto \boldsymbol{\sigma} \cdot \mathbf{k}$, where $\boldsymbol{\sigma}$ is Pauli matrix in vector form. Most of massless fermions are neutral; however, electrons in Dirac materials are charged massless particles and can be easily influenced by external magnetic or electric fields (this is known as field effect). This unique property has a great potential to be exploited in future electronic applications such as single molecule gas detection, transistors, integrated circuits, ultra capacitors, and bio devices.

1.3 Other 2D Materials

Based on the bulk material used to create 2D materials, they can be classified into two main classes: 1) Van der Waals 2D materials and, 2) layered ionic solids. Van der Waals 2D materials are the most common form [15]. These materials are created by mechanical or chemical exfoliation of their bulk material. The bulk of these materials are stacked layers arranged with van der Waals forces (hence their name) [11]. The examples of these kind of 2D materials are graphene which is one layer of graphite, hexagonal boron nitride[16], and phosphorene[17], which is one layer of black phosphorus. Graphene and phosphorene have strong covalent bonds between atoms in one layer. The atomic bonds in each layer can also be ionic. Due to weak van der Waals interaction between layers, these solids can be easily exfoliated. Metals (M) such as titanium, zirconium, hafnium, vanadium, niobium, and tantalum with chalcogens (elements in group six of the periodic table) — mostly sulfide, tellurium and selenium (usually labeled X) — are the most common and studied form of other van der Waals 2D materials with chemical formula MX_2 . MoS_2 [18], TiSe_2 and WSe_2 are examples of this type.

The second class of 2D materials is called layered ionic solids [19]. The atoms in a single layer of these materials are bond together with strong electrostatic bonds. Most of these 2D materials are metallic oxides, for instance TiO_2 , WO_3 , MnO_2 and $\text{Ni}(\text{OH})_2$.

1.4 Properties of 2D Materials

In 2D materials, electrons are confined in a surface rather than a 3D space. The interaction between layers of bulk materials plays a significant role in their electronic and optical properties [20]. By confining interactions to two dimensions, new electronic behavior is observed (such as Hall effects) which has made researchers optimistic to exploit these properties and make new electronic devices. Another difference of 2D materials compared to bulk 3D materials is the effect of shape and stacking on their properties. For example, the properties of a single layer of graphene are different from those of 2 layers and they are still different from 3 layers of graphene stacked together [21]. By stacking more layers of graphene together the properties are similar to the bulk form which is graphite. Even relative stacking angles play a role in electronic properties¹⁷. Deformation also changes the properties. For instance, strain changes the properties by altering the orbital hybridization [1].

The other important feature of 2D materials is their high surface-to-volume ratio. In 2D materials there are numerous atoms that are considered surface atoms. Therefore 2D materials are membranes exposed to their environment and very sensitive to changes in such environment. Consequently, 2D materials are potentially good materials for sensing [22].

Geometry of 2D Materials

1.5 Deformation in 2D Materials

In the previous section it was mentioned that the shape of 2D materials alters their properties. Graphene is the most popular 2D material and the subject of extensive research. Much research has also been done on graphene and the effect of strain in electronic properties [4, 23]. Graphene is amenable to external forces and, with a very high Young's modulus, can withstand up to 30 percent strain [24]. In addition to these unique properties are influenced by external exerted strain [4, 23, 25]. The possibility of modifying the electronic properties by applying a strain pattern has triggered extensive research and novel ideas on the issue. Two-dimensional materials accept deformation that increase bonds by up to 20% before mechanical failure (fracture); this level of deformation is unheard of in 3D form of these (bulk) materials.

The change in crystal lattice of graphene can be classified into four ways [25]:

- 1- Strain changes the distance between atoms and, consequently, the shape of chemical orbitals changes.
- 2- Modifying the distance between nearest neighbor atoms leads to change in sub-lattices and hopping parameter [25] therefore non-diagonal elements in Dirac equation will change. This effect is similar to inducing a gauge field on the lattice [25].
- 3- By substituting hexagons in the lattice with pentagons and heptagons one can exert large deformations in which pentagons add convex deformation and heptagons adds concave deformation to the graphene changes [3].
- 4- Deformation on graphene membrane changes the distance between π and σ orbitals which causes overlapping and hybridizing of these orbitals [3].

These generic observations apply (with some exceptions and modifications) to other 2D materials.

1.6 Lack of Accuracy of Continuum Mechanics for 2D Materials

In the existing theories, explaining the deformation of 2D materials tends to consider them as continuous membranes. That is, a continuous deformation field $\mathbf{u}_\alpha(\xi^1, \xi^2)$, in two dependent directions ξ^1 and ξ^2 , is considered. In thin plate elasticity theory [2, 26] the deformation field can be expressed as a strain field in the following way:

$$u_{\alpha\beta} = \frac{\partial u_\beta}{\partial \xi^\alpha} \frac{\partial u_\alpha}{\partial \xi^\beta} + \frac{\partial u_\beta}{\partial \xi^\alpha} \frac{\partial u_\alpha}{\partial \xi^\beta} + \frac{\partial z}{\partial \xi^\alpha} \frac{\partial z}{\partial \xi^\beta} \quad (\text{Equation 4})$$

in which z is the deformation normal to the membrane[4], and α, β are integers between 1 and 2.

The local geometry of a surface embodied in 3D space is determined using four invariant numbers from the metric and curvature tensors, which indicates how much the surface is stretched and curved under a deformation compared to a reference unreformed conformation. Appropriate invariants are: 1) the trace of metric tensor; 2) the determinant of metric tensor; 3) the product of principal curvature, which is called the Gaussian curvature; and, 4) the sum of the two principal curvatures (the mean curvature). These concepts and parameters are discussed in following pages.

Within the continuum frameworks the mechanics of the membrane and its geometry are dynamically related by (thin plate first order continuum elasticity theory):

$$g_{\alpha\beta} = \delta_{\alpha\beta} + 2u_{\alpha\beta} \ , \quad k_{\alpha\beta} = \hat{n} \cdot \frac{\partial g_\alpha}{\partial \xi^\beta} \ , \quad (\text{Equation 5})$$

in which $g_{\alpha\beta}$ is the metric tensor, which describes how the local vicinity is stretched with respect to a “reference” metric for an undeformed body, $\delta_{\alpha\beta}$. The curvature tensor, $k_{\alpha\beta}$, tells us the local curvature at a given point and $g_\alpha = (\xi^1, \xi^2)$ is the tangent field to the membrane at any given point. The local normal to the 2D continuum manifold is shown by \hat{n} and it can be found by:

$$\frac{\begin{matrix} \rightarrow & \times & \rightarrow \\ g_{\xi^1} & & g_{\xi^2} \end{matrix}}{\left| \begin{matrix} \rightarrow & \times & \rightarrow \\ g_{\xi^1} & & g_{\xi^2} \end{matrix} \right|} \quad (\text{Equation 6})$$

More on the continuum geometry will be covered later. The main point here is that the continuum theory applies to slow and homogeneous deformations. Thus, deformations observed in practice, for instance, the formation of ripples in 2D materials, may not be properly described by first-order continuum mechanics. These limitations require researchers to study an exact method for discussing the geometry of 2D crystals directly from atoms [4, 27]. The exact method used to tell shape introduced here is a recent mathematical language known as discrete differential geometry [3, 4, 28].

1.7 Discrete Geometry Framework

2D materials can be easily embedded into 3D space. The surface of these 2D materials is not a continuum because these structures are created by discrete points (atoms) and lines (chemical bonds). A path on the lattice can be considered as a sequence of vectors which creates a multi-broken line, and the surface can be considered as a collection of many finite hexagonal planes, therefore the surface of 2D materials surface is discrete. Consequently, it becomes interesting to investigate if there are exact alternative, precise, concepts to determine the shape.

1.7.1 Differential Geometry Concepts

In this section essential concepts of differential geometry are discussed.

Curvature and curvature tensor: Consider a curve in 2D space $y = f(x)$. The first information known about the shape of the curve is the tangent line to each point. The local tangent line is given by the first derivative of the curve. The second piece of information of the curve is its local curvature which is related to the second derivatives. In a 2D space this two parameters are sufficient to know the local shape of the curve.

Curvature is the reciprocal of the radius of an osculating circle on a given point as shown in Figure 2.

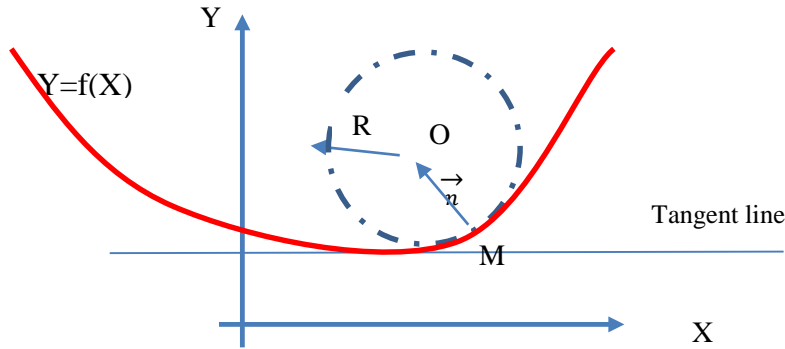


Figure 2. Osculating circle and tangent line.

Therefore, the curvature k at point M is given by:

$$k = \frac{1}{R}. \quad (\text{Equation 7})$$

In 3D space the shape of the curve needs another component called torsion. Consider a curve $= f(t)$:

- \mathbf{T} the tangent vector in each point is defined as $\mathbf{T} = \frac{d\mathbf{r}}{ds}$.

- \mathbf{N} is the normal vector to the curve in each point and it is defined by: $\mathbf{N} = \mathbf{R} \times \frac{d\mathbf{T}}{ds}$.
- \mathbf{B} is the cross product of tangent vector and Normal vectors: $\mathbf{T} \times \mathbf{N}$.

Where s is length of the curve $f(t)$, and \mathbf{R} is the radius of osculating circle. These three vectors (\mathbf{T} , \mathbf{N} , and \mathbf{B}) build a useful local frame to discuss curves in 3D.

Curvature of a surface embedded in space: Unlike the curvature discussed in previous section, the curvature of surfaces is not a single scalar value because, by looking at Figure 3, there are infinite numbers of circles that are tangential to the surface at any given point. In this situation,

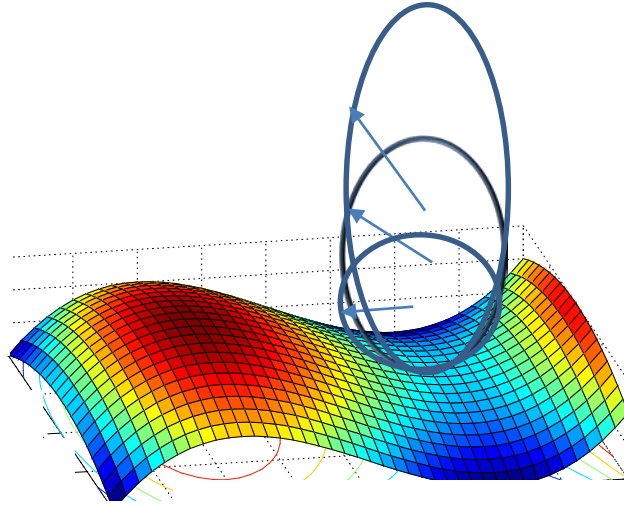


Figure 3. Different osculating circles tangent to a saddle surface in one point.

the maximum and minimum curvature of all osculating circle on a point are called principal curvatures in that point. Said another way, the curvature on a surface in 3D space is a tensor with two principal eigenvalues known as the principal curvatures. The two circles are defined taking extreme radii. The invert of these two (principal) radii are known as principal curvatures ($k_1 = \frac{1}{r_1}$, $k_2 = \frac{1}{r_2}$). The two principal curvatures are related to the mean curvature (H) and the Gaussian curvature (K) by a simple formula [29]:

$$k_1 = H - \sqrt{H^2 - K} \ , \quad k_2 = H + \sqrt{H^2 - K} \quad (\text{Equation 8})$$

By having four parameters — The Gaussian curvature, K , the mean curvature, H , the determinant, and the trace of metric tensor (Equation 5) — the geometry of a continuum 2D surface can be determined.

First fundamental form and metric tensor: For surface with equation $M = f(x(u, v)) \ , y(u, v), h(u, v)$, then, the metric tensor of this surface is written as [29]:

$$g_{ij} = \begin{pmatrix} E & F \\ F & E \end{pmatrix} = \begin{pmatrix} \frac{\partial f}{\partial u} \cdot \frac{\partial f}{\partial u} & \frac{\partial f}{\partial u} \cdot \frac{\partial f}{\partial v} \\ \frac{\partial f}{\partial v} \cdot \frac{\partial f}{\partial u} & \frac{\partial f}{\partial v} \cdot \frac{\partial f}{\partial v} \end{pmatrix}. \quad (\text{Equation 9})$$

This tensor is called a metric tensor because it is related to calculating distances on a curve constrained to the surface. From this definition, a differential curve length on the surface can be written as:

$$ds^2 = Edu^2 + 2Fdudv + Gdv^2. \quad (\text{Equation 10})$$

For example, in a Cartesian Euclidean system:

$$ds^2 = \mathbf{du}^2 + \mathbf{dv}^2. \quad (\text{Equation 11})$$

That means, two vectors \mathbf{du}, \mathbf{dv} are orthogonal so $F=0$, and \mathbf{du}, \mathbf{dv} are of unit length so $E=G=1$, and, therefore the metric tensor can be easily computed by:

$$g_{ij} = \begin{pmatrix} 1 & 0 \\ 0 & 1 \end{pmatrix}. \quad (\text{Equation 12})$$

Analytical Gaussian curvature: Suppose the surface has a function $S = f(x, y, z(x, y))$. The Gaussian curvature can be computed by Equation 13:

$$K = \frac{z_{xx}z_{yy} - z_{xy}^2}{(1 + z_x^2 + z_y^2)^2}. \quad (\text{Equation 13})$$

Curvature for a Gaussian bell: Using this equation Gaussian curvature of a Gaussian bump is calculated. It is easier to deal with the Gaussian bump in cylindrical coordinates. The Gaussian and the mean curvatures are calculated below [4]:

$$z(r) = A \exp\left(-\frac{r^2}{2\sigma^2}\right), \quad (\text{Equation 14})$$

$$z_r = \frac{-rA}{\sigma^2} \exp\left(-\frac{r^2}{2\sigma^2}\right) \quad (\text{Equation 15})$$

$$z_{rr} = \frac{-r^2A}{\sigma^4} \exp\left(-\frac{r^2}{2\sigma^2}\right) + \frac{A}{\sigma^2} \exp\left(-\frac{r^2}{2\sigma^2}\right) \quad (\text{Equation 16})$$

$$k_1 = \frac{z_{rr}}{(1 + z_r^2)^{\frac{3}{2}}}, \quad k_2 = \frac{z_r}{r\sqrt{1 + z_r^2}} \quad (\text{Equation 17})$$

$$K = k_1 k_2 = \frac{z_{rr} z_r}{r(1 + z_r^2)^2} \quad (\text{Equation 18})$$

$$H = \frac{1}{2}(k_1 + k_2) = \frac{1}{2} \left(\frac{z_{rr}}{(1 + z_r^2)^{\frac{3}{2}}} + \frac{z_r}{r\sqrt{1 + z_r^2}} \right) \quad (\text{Equation 19})$$

in which A and σ are constants, r is the distance from the origin (middle of the Gaussian bump),

k_1 and k_2 are principal curvatures, K is the Gaussian curvature and H is the mean curvature.

Analytical Gaussian curvature (K) of the previously mentioned Gaussian bump is calculated

using Equations 18 and 19 for $A = 10 \text{ \AA}$ and $\sigma = 15 \text{ \AA}$. and shown in Figure 4.

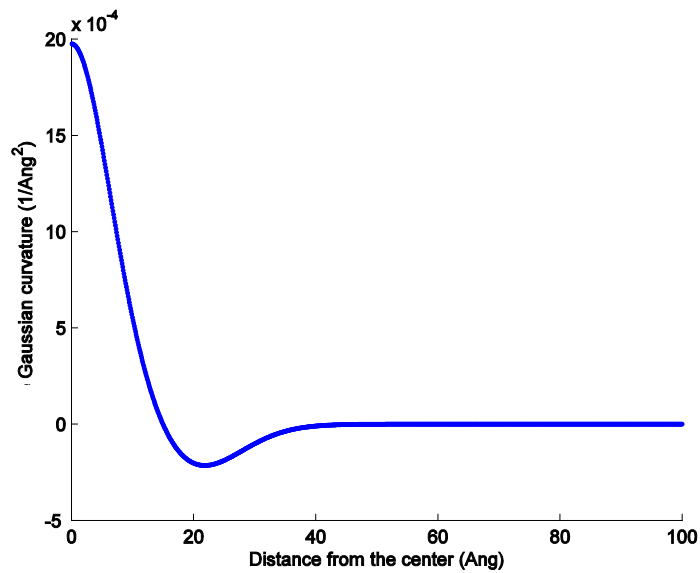


Figure 4. Analytical Gaussian curvature of a Gaussian bump.

Analytical mean curvature (H) of the Gaussian bump is calculated and shown in Figure 5.

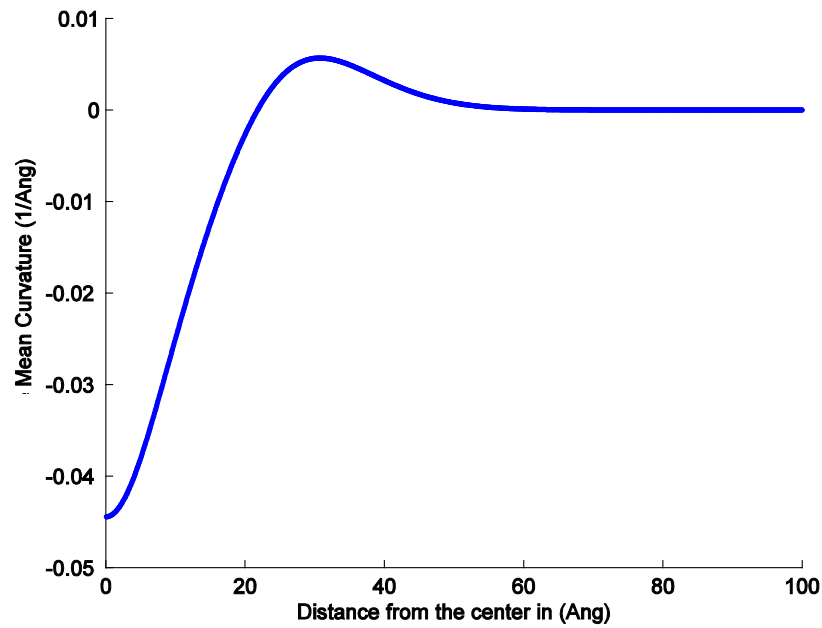


Figure 5. Analytical mean curvature for a Gaussian bump.

Gaussian curvature: Instead of using two principal curvatures as two significant parameters in discussing shapes, the Gaussian (K) and mean curvatures (H) can be used. The Gaussian curvature is the product of the two principal curvatures. The Gaussian curvature divides surfaces into three classes. These three classes are shown in Figure 6 and discussed in the following.

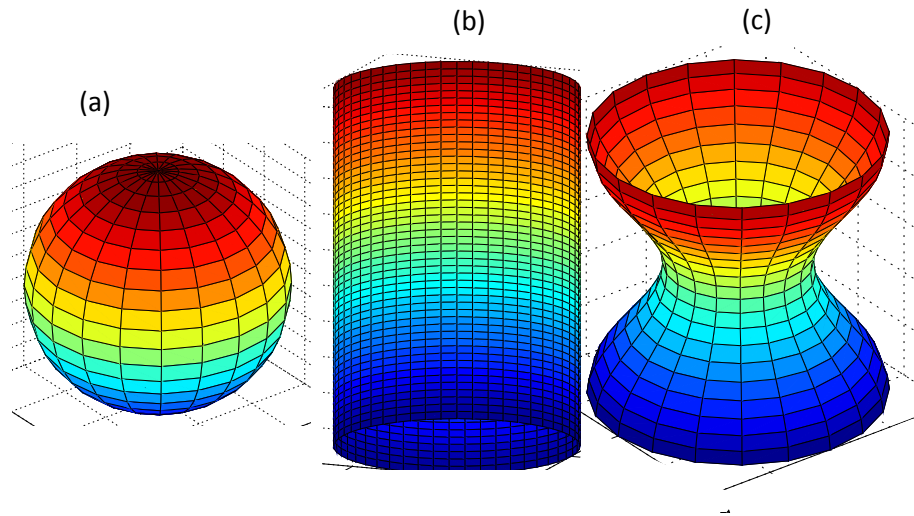


Figure 6. Surface with (a) positive, (b) negative and (c) zero Gaussian curvature.

surfaces with positive Gaussian curvature, such as a sphere, Figure 6(a);

- surfaces with zero Gaussian curvature which is caused by one principal curvature going to zero (examples of these surfaces are planes, cones and cylinders) Figure 6(b); and,
- surfaces with negative Gaussian curvature where one principal curvature is negative and the other one is positive (an example of this kind is a saddle surface or a “pringles potato chip”), Figure 6(c).

Mean curvature: The mean curvature (H) is the average of the two principal curvatures on a surface. From algebra, the sum of principal eigen-values of a matrix is the equal the trace of the matrix. The trace of the matrix can be added to calculate the mean curvature.

Geodesic: In a planar surface, the shortest path between two points is a straight line connecting them. A geodesic is a concept that generalizes this idea to curved surfaces (manifolds). Earlier, geodesy was used to measure the shortest path between two points on the Earth. On a circle, the shortest distance between two points is the smaller arc that is part of the great circle on the surface that connects the two points. By looking at this in Figure 7, it may be understood that the

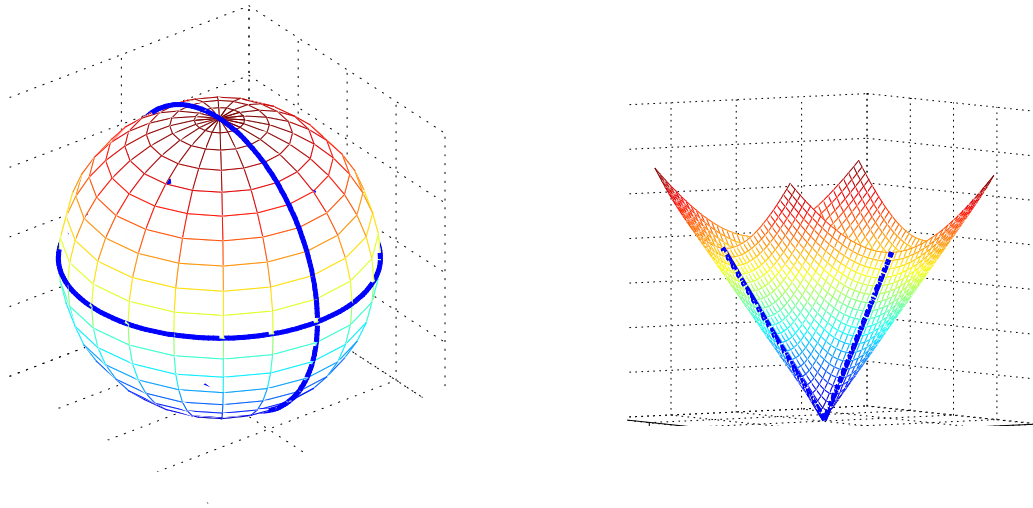


Figure 7. Geodesic curve on different surfaces.

local curvature in each point of the great circle is parallel to the surface of the sphere. In other more complex surfaces, the geodesics are defined as the shortest path between two points, and the local curvature in each point of the curve is parallel to the normal vector on that point.

Geodesic curvature: The curvature of a curve that is restricted to a 2D surface can be divided into two components. One component is parallel to the normal of the surface which is equal to the curvature of geodesic curvature going through that point, and the second component is tangent to the surface (as in a finite boundary). The component that is normal to the surface is called geodesic curvature, for instance in a sphere the geodesic curvature is equal to the curvature of the great circle on the sphere.

Departing altogether from this view of surfaces as continuum objects, the discrete character of atomistic surfaces is discussed next.

1.7.2 Discrete Differential Geometry Concepts

Angle defect: The sum of all angles is equal 360 degrees on a plane, but if one vertex moves to the third direction, the summation is not 360 degrees anymore. Figure 8 depicts a Bucky ball which represents C_{60} . The sum of shown angles in closed path on the Figure is not 360 degrees. And the deviation from 360 degrees is precisely the angle defect.

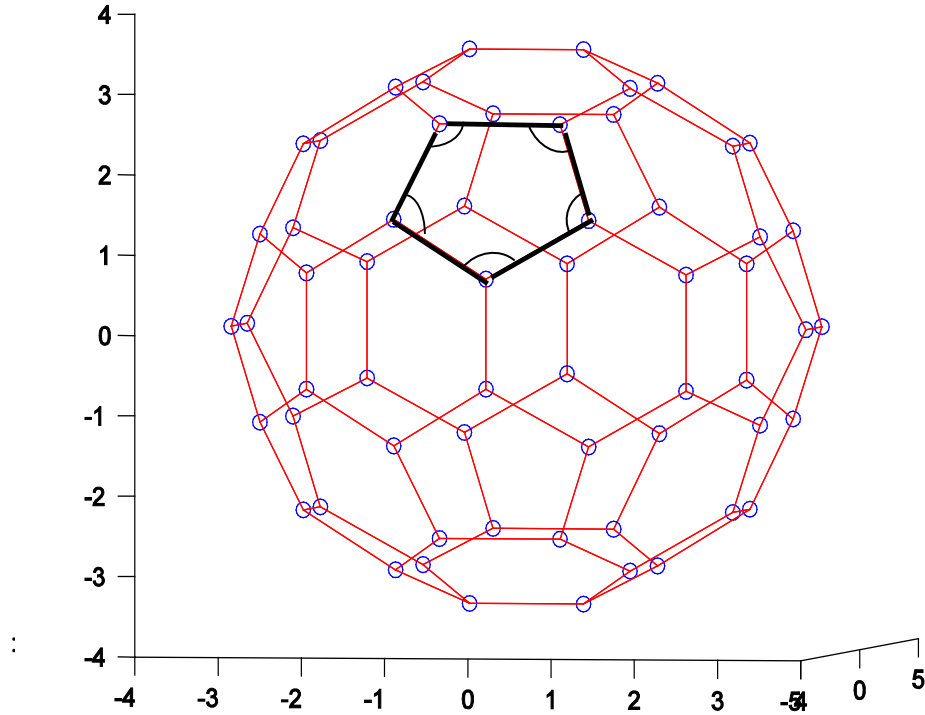


Figure 8. Buckyball; the sum of all internal angles of a pentagon embedded on a surface deviates from 360 degrees (scales in angstroms).

Voronoi tessellations: A Voronoi tessellation is a method for subdividing a plane with many vertices into spaces. Around each vertex, the locus of all points that are closer to the central vertices is sought. The total subdividing spaces are called Voronoi tessellations (this concept is known as Wigner-Seitz unit cells in condensed matter physics) [30, 31]. The vertices are called

seeds, and the lines joining seeds are called edges (for this work, seeds will be atomic positions, and edges will be covalent bonds). The two example of a Voronoi tessellation are presented in Figure 9. Delaunay finding is another concept in triangulation in which the space is subdivided into triangles in which none of the vertices locates in the circumcircle of other triangles. This triangulation optimizes the angles of triangles to avoid skinny triangles that have acute angles.

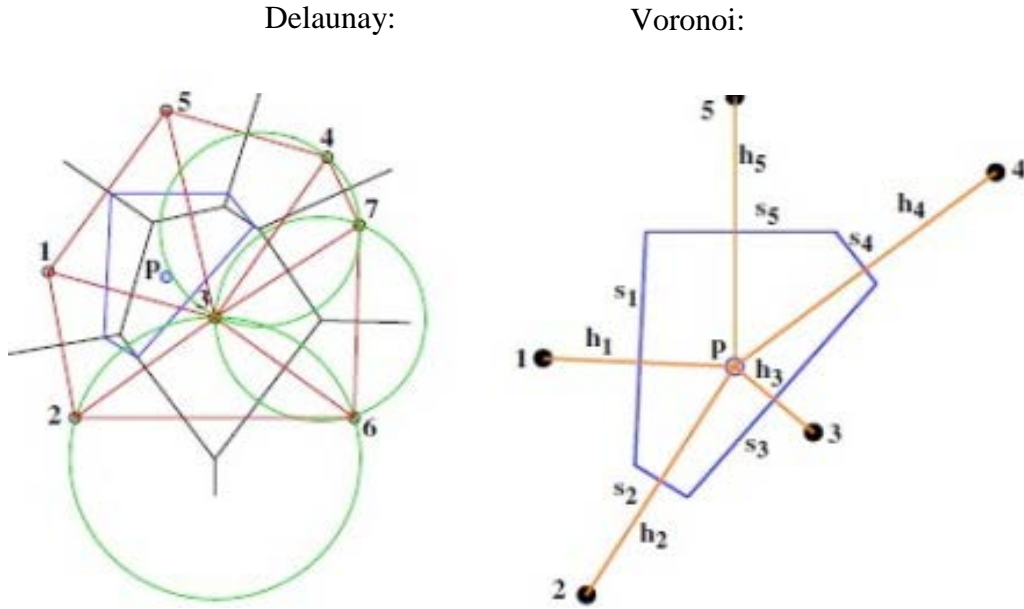


Figure 9. Delaunay triangulation and Veronoi tessellation for an effective surface in Gauss-Bonnet theory [31].

Gauss Bonnet theorem and the Gaussian curvature: One of the fundamental theorems of discrete differential geometry which relates the Gaussian curvature to the geodesic curvature, the discrete area of surface, and to the number of significant defects in the topology, is the classic Gauss-Bonnet theorem:

$$\iint_A K dA + \oint_{\partial A} k_g ds - \sum_1^n \alpha_i = 2\pi\chi(A), \quad (\text{Equation 20})$$

in which K is the Gaussian curvature, A is the area of the discrete surface, k_g is the geodesic curvature which is the trajectory of curvature in the tangent plane. α_i is the external angle between various curves that create the boundary of the surface A . $\chi(A)$ is the Euler number and it refers to the number of major defects in the surface. For a surface without any hole $\chi(A)$ is 1, and for a torus $\chi(A)$ is equal to 2. The Gauss- Bonnet theorem in a boundary-free surface yields an equation which gives us the Gaussian curvature on a discrete surface. As indicated in Figure 10, many lines are creating the boundaries of discrete surface A , and because the geodesic

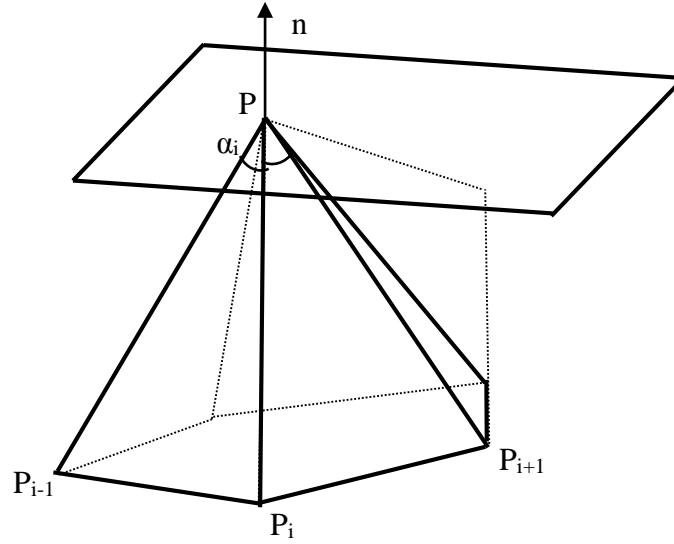


Figure 10. Six vertices, one out of plane. Edges and angles that are needed to find discrete curvature [26].

curvature k_g of lines is zero, the second term in the left side of the Equation 20 is zero.

Moreover for a polyhedra the sum of external angles is equal to the sum of interior angles between edges that connect central point to the neighbor atoms. Therefore, the Gauss- Bonnet theorem for a polyhedra with six sides reduces to:

$$2\pi - K_p = \sum_{i=1}^6 \theta_i \quad (\text{Equation 21})$$

In which K_p is the dimensionless angle defect. To compute Gaussian curvature, K_p should be divided by the area of the Voronoi unit cell A_p . Voronoi area is locus of points that their distance

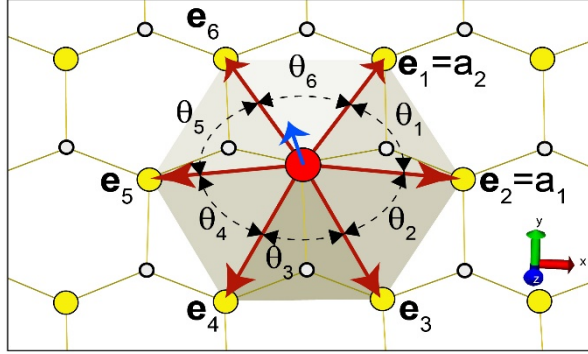


Figure 11. Atoms required to calculate Gaussian and mean curvature for hexagonal lattices.

to the center point p is less than the distance to any other points. For graphene, silicone, hexagonal boron nitride, and blue phosphorus, this geometry is depicted in the Figure 11,

Therefore:

$$K_D = \frac{K_p}{A_p}, \quad (\text{Equation 21})$$

where “D” stands for discrete. Note that K_D has units of $\frac{1}{L^2}$ with L standing for length, as it should.

Discrete approach to calculate Gaussian and mean curvatures: Many more in depth approaches are presented in literature [32]. In the following some of those methods are presented.

The popular method of estimating Gaussian curvature is using angle defect. Referring to Figure 10 the angle defect can be presented as:

$$2\pi - \sum_i \theta_i \quad (\text{Equation 22})$$

And the Gaussian curvature can be estimated as a fraction of this angle defect.

$$K = (2\pi - \sum_i \theta_i) \times \frac{1}{F}, \quad (\text{Equation 23})$$

where K is the Gaussian curvature and F is a parameter related to area. Different approaches are used to estimate F . In Figure 10, point P is surrounded by neighbor points P_1, P_2, \dots, P_i . The angle between P_i, P , and P_{i+1} is showed as θ_i , and the area of the triangle P_iPP_{i+1} is shown as A_i .

Formula1: A popular method is to estimate F with the sum of areas of all triangles with the form of P_iPP_{i+1} divided by 3[33].

$$K = 3 \times \frac{2\pi - \sum_i \theta_i}{\sum A_i} \quad (\text{Equation 24})$$

Formula 2: Another method is to estimate parameter F in equation (23) with S_p which is calculated as:

$$S_p = \sum \frac{1}{4\sin\theta_i} \left[\eta_i \cdot \eta_{i+1} - \frac{\cos\theta_i}{2} (\eta_i^2 + \eta_{i+1}^2) \right] \quad (\text{Equation 25})$$

Parameter S_p is called module of mesh at Point P .

Formula 3: By modifying the first approximation given by Equation (23) a more accurate estimate for Gaussian curvature:

$$K = \frac{2\pi - \sum_i \theta_i}{\frac{1}{2} \sum A_i - \frac{1}{8} \sum \cot(\theta_i) \times d_i^2} \quad (\text{Equation 26})$$

Where d_i^2 represents the square of the distance between P and P_i .

Formula 4: There is another formula which is based on Voronoi areas.

$$K = \frac{2\pi - \sum_i \theta_i}{A_M(p)}, \quad (\text{Equation 27})$$

where, $A_M(p)$ is the Voronoi area. The area of triangles created by edges from point p to p_i can be approximated by Voronoi area.

Formula 5: All of the formulas presented before are applicable to polyhedrals with at least 6 edges, which means the Gaussian curvature has to be written based on the position of 6 vertex around it. The formula 28-29, converges the curvature for at least 5 vertices:

$$K = \frac{2\pi - \sum \gamma_i - 2(S_p - A) \times H^2}{2A - S_p}. \quad (\text{Equation 28})$$

Here:

$$A = \sum \frac{1}{4 \sin \gamma_i} \left(\frac{\eta_i \eta_{i+1}}{2} (1 - \cos 2\varphi_i \cos 2\varphi_{i+1}) - \frac{\cos \gamma_i}{4} (\eta_i^2 \sin^2 \varphi_i - \eta_{i+1}^2 \sin^2 \varphi_{i+1}) \right), \quad (\text{Equation 29})$$

In which η, φ, γ are angles and shown in Figure 10.

Mean curvature: the discrete mean curvature is a vector. Suppose v_i is the location of the point i on the surface A depicted in Figure 10 and v_p is the location of central atom p , then one can calculate the edge which connects these two points together, $e_i = v_i - v_p$, and by considering $n_{i,i+1}$ as the normal vector to edges e_i and e_{i+1} , the mean curvature can be computed as the following equation:

$$H_D = \sum_{i=1}^6 \frac{e_i \times (n_{i,i+1} - n_{i,i-1})}{4A_p} \quad (\text{Equation 30})$$

Mean curvature calculation: the mean curvature can also be obtained by a popular formula presented and proved by Xu, and Pinkall [32, 34].

$$H = 2 \left\| \frac{\sum (\cot \alpha_i + \cot \delta_i) \mathbf{e}_i}{\sum (\cot \alpha_i + \cot \delta_i) \eta_i^2} \right\|, \quad (\text{Equation 31})$$

in which α_i , δ_i , η_i^2 , \mathbf{e}_i are shown in Figure 10. Nevertheless the Equation 27 were used on this work.

Trace and determinant of metric tensor: the metric tensor can be computed as an inner (“dot”) product of lattice vectors, the determinant of the metric tensor is an indication of the stretch between bonds. The trace of the metric tensor which is the sum of eigenvalues can be easily computed by adding up the main diagonal elements.

1.8 Metric Computation for Different Lattices

A metric must be positive-definite ($g_{\alpha\alpha} > 0$) and symmetric ($g_{\alpha\beta} = g_{\beta\alpha}$). The metric of 2D lattice with only one layer like graphene, are computed by a “dot” product of lattice vectors. Consider \mathbf{a}_1 and \mathbf{a}_2 are two lattice vectors the metric tensor is found as:

$$g_{\alpha\beta} = \begin{pmatrix} \mathbf{a}_1 \cdot \mathbf{a}_1 & \mathbf{a}_1 \cdot \mathbf{a}_2 \\ \mathbf{a}_2 \cdot \mathbf{a}_1 & \mathbf{a}_2 \cdot \mathbf{a}_2 \end{pmatrix}, \quad (\text{Equation 32})$$

which satisfies the two properties of a metric indicated above.

For other lattices which has a thickness more than one atom, like black phosphorus, AlP and Bi_2Se_3 , in addition to these two lattice vectors another vector which has a component normal to these two vectors and with the length equal to the thickness d was considered. The metric tensor for these lattice structures is thus:

$$g_{\alpha\beta} = \begin{pmatrix} \mathbf{a}_1 \cdot \mathbf{a}_1 & \mathbf{a}_1 \cdot \mathbf{a}_2 & \mathbf{a}_1 \cdot \mathbf{d} \\ \mathbf{a}_2 \cdot \mathbf{a}_1 & \mathbf{a}_2 \cdot \mathbf{a}_2 & \mathbf{a}_2 \cdot \mathbf{d} \\ \mathbf{a}_1 \cdot \mathbf{d} & \mathbf{a}_2 \cdot \mathbf{d} & \mathbf{d} \cdot \mathbf{d} \end{pmatrix} \quad (\text{Equation 33})$$

in which \mathbf{a}_1 and \mathbf{a}_2 are lattice vectors and \mathbf{d} is thickness.

Discrete Curvature and Metric Calculation for Various Lattices

The discrete geometry has been introduced in previous sections; it will now be applied to 2D materials. Since there are structural differences among unit cells for different 2D materials (i.e., hexagonal versus square or rectangular unit cells) changing the neighboring vertices from which local Gaussian and mean curvatures are obtained was required. Therefore, for each of these 2D materials mentioned in previous section, certain points were defined to calculate curvature.

Hexagonal Lattice: For computing the Gaussian and mean curvature in each point of the hexagonal lattice like graphene and hexagonal boron nitride at least six neighbor atoms are needed [32]. Trying to tell the curvature based on only nearest neighbors in hexagonal unit cells is not possible because each atom in the hexagonal lattice only has three nearest neighbors. Therefore the second nearest neighbors should be used. For hexagonal structures six second nearest neighbors shown in Figure 11 were used, and by computing edges, triangle areas, and angle between the Gaussian and mean curvature were obtained using Equations 27 and 30.

Square lattice as in aluminum phosphide: At least six neighboring atoms are needed to carry out the discrete computation. For this structure, eight second nearest neighbors were used as shown in Figure 12.

Curvature computation for multi-layer 2D materials: The number and position of atoms that were used to calculate the Gaussian and mean curvature for multi-layered materials are similar to single-layer materials, because curvature were calculated based on the central layer.

Curvature computation in the presence of defects: Defects make it necessary to generalize the model to discuss shape. For example, atomistic defects are made by replacing hexagonal shapes with heptagons and pentagons. Pentagons induce positive Gaussian curvature to the structure,

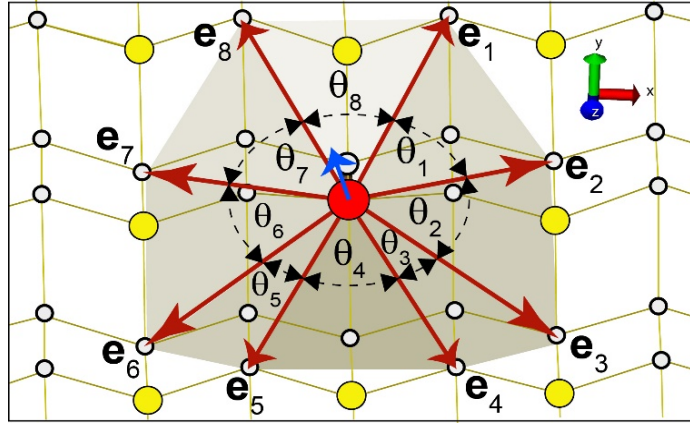


Figure 12. Atoms required to calculate Gaussian and mean curvature for a square lattice.

while heptagons load negative Gaussian curvature to the structure. The number of nearest neighbors that are used to compute the curvature, depends on heptagonal or pentagonal defects. Defects and required vertices to calculate curvature are shown in Figure 13.

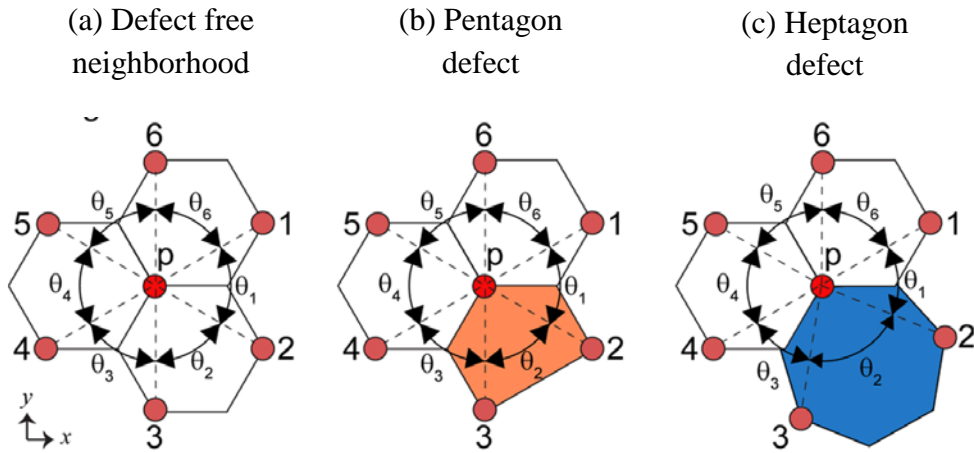


Figure 13. Required atoms for calculating Gaussian and mean curvature in presence of defects in a hexagonal lattice [4].

Building Structural Models:

In the following, a novel method for discussing the geometry of 2D materials is applied. This was done for different structural lattices, such as hexagonal ones with non-zero thickness, square and other peculiar lattices, such as black phosphorus.

The first step for studying the geometry of 2D crystals is building their structures under a deformation. This should require a mechanical model that informs the atoms where to go as a deformation is enforced. This mechanical model can have different degrees of precision, and it could be directly informed by density-functional theory (DFT).

The study of 2D materials is only ten-years old. Full-scale DFT calculations are out of the question, and reliable force fields are yet to be crafted for many of the 2D materials that were studied here. This, however, should not stop the determination of fundamental frameworks to inquire about shape.

A mechanical model was devised for the deformation that was calculated from density-functional theory. The deformation is based upon a model with a number of approximations. The materials were stretched in the 2D-plane, and the final atomic positions were recorded upon relaxations. Poisson law states that an in-plane elongation will lead to an out-of-plane contraction of magnitude σ (this is usually known as Poisson ratio). The contraction is reported in the second row on Tables 1-5; the equilibrium values are shown by bold font in the tables. This information was used to build a rudimentary mechanical model.

The 2D materials were adopted to the shape of the Gaussian bell discussed on page 13 which means, the z-position for each atom increases by z as given in Equation 14. This simplifies direct contrast between the predictions of continuum and discrete geometrical theories.

For material with non-zero thickness (WSe₂, Bi₂Se₃, silicene, AIP, black phosphorus), upper layers must contract their relative height because the material stretches when conforming to the Gaussian bump. The amount of stretching is extracted from the average increase of the local lattice vectors upon deformation via a linear fit from data in Tables 1-5.

The reference unit cell parameters such as lattice vectors, basis vectors and lattice constants were computed by DFT structural relaxations. The structural relaxation was performed using VASP software. The reference planar configuration of atoms were built by using structural parameters found from VASP calculation. The resulting structural models are shown in the following sections.

1.9 Hexagonal Boron-Nitride

Hexagonal boron-nitride (HBN) shown in Figure 14, is a structure that consists of boron and nitrogen atoms at A and B sub-lattices, respectively. The structure of bulk HBN is similar to graphite. Multiple layers of HBN are stacked together with weak ionic interaction between

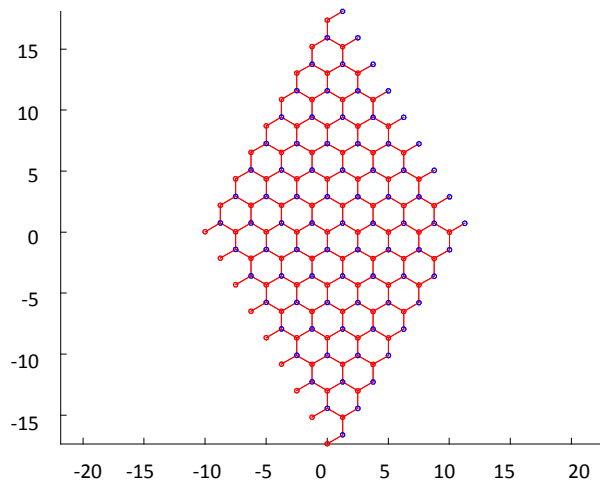


Figure 14. Hexagonal boron nitride lattice (units in angstroms).

layers, while boron atoms are joint to nitrogen by covalent bonds. HBN has a large semiconducting band gap equal to 5.5 eV.

Structural parameters: In each HBN unit cell there are two atoms. The positions of these atoms are given below by basis vectors which are shown in Equations 33-36. The lattice vectors of HBN are similar to those of graphene. Lattice vectors in angstroms are shown by \mathbf{v} and atomic basis in a lattice are depicted by \mathbf{b} .

$$\mathbf{v}_1 = (2.34, \quad - 4.05, \quad 0.00), \quad (\text{Equation 33})$$

$$\mathbf{v}_2 = (2.34, \quad 4.05, \quad 0.00), \quad (\text{Equation 34})$$

$$\mathbf{b}_1 = (0.00, \quad 0.00, \quad - 0.43), \quad (\text{Equation 35})$$

$$\mathbf{b}_2 = (2.34, \quad 1.35, \quad 0.43), \quad (\text{Equation 36})$$

Applying Deformation to the Planar Structure: For calculation of geometrical parameter a deformed membrane is needed. As was previously discussed, a known Gaussian deformation is enforced on atoms. The new atomic coordinates have a different height compared to planar

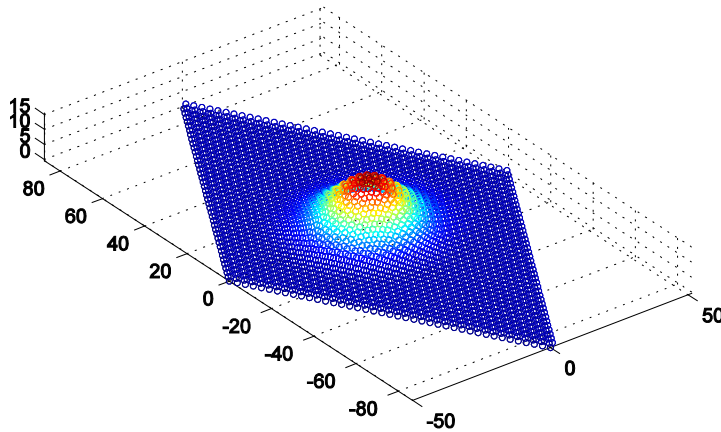


Figure 15. Gaussian deformation applied to hexagonal boron nitride (units in angstroms).

structure which is shown in Figure 15. For local curvature computation in each point, the coordinates of six nearest vertices were used as shown in Figure 11.

1.10 Low-Buckled Silicene

The structure of low-buckled silicene is hexagonal, however, on any other sub-lattice, atoms are shifted (i.e., they “buckle out of plane”) in the third direction. The structure is shown in the Figure 16.

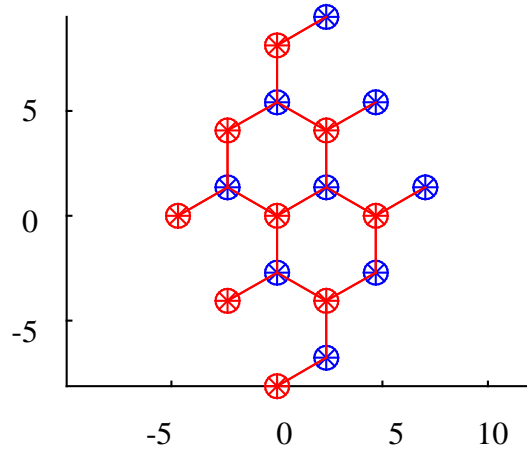


Figure 16. Low buckled silicene structure (units in angstroms).

The lattice vectors and atomic position of this material were calculated by structural relaxation. The data is presented in the following equations.

$$\mathbf{v}_1 = (2.34, 4.05, 0.00), \quad (\text{Equation 37})$$

$$\mathbf{v}_2 = (2.34, -4.05, 0.00), \quad (\text{Equation 38})$$

$$\mathbf{b}_1 = (0.00, 0.00, -0.43), \quad (\text{Equation 39})$$

$$\mathbf{b}_2 = (2.34, 1.35, 0.43), \quad (\text{Equation 40})$$

1.11 Aluminum Phosphate

AIP has a buckled square lattice. The middle layer consists of Al atoms with P atoms joined below and down the middle layer. The relaxed structural parameters, lattice vectors, and basis vectors is presented in following equations (in angstroms):

$$\mathbf{v}_1 = (3.95, 0.00, 0.00), \quad (\text{Equation 41})$$

$$\mathbf{v}_2 = (0.00, 3.95, 0.00), \quad (\text{Equation 42})$$

$$\mathbf{b}_1 = (0.00, 0.00, 0.00), \quad (\text{Equation 43})$$

$$\mathbf{b}_2 = (1.97, 1.97, 0.00), \quad (\text{Equation 44})$$

$$\mathbf{b}_3 = (0.00, 1.97, 1.35), \quad (\text{Equation 45})$$

$$\mathbf{b}_4 = (1.97, 0.00, -1.35), \quad (\text{Equation 46})$$

As discussed before, any deformation exerted on AIP lattice will cause a change in actual thickness of the 2D material. This thickness which can be defined by the distance between the two outer layers can be found as a function of lattice constant. By performing relaxation in a unit cell and changing the lattice constant, the optimum thickness was computed and given in Table 1.

Table 1. Thickness results from VASP for AIP.

Lattice constant (Å)	3.25	3.45	3.65	3.95	4.05	4.25	4.45	4.85	5.25
Thickness (Å)	1.61	1.55	1.49	1.35	1.31	1.19	1.03	0.407	0.0014

Table 1 was used to compute the thickness change after applying Gaussian deformation field. The change in thickness reflects the dimensional change due to stretching.

The shape of the AIP lattice is shown below from different views.

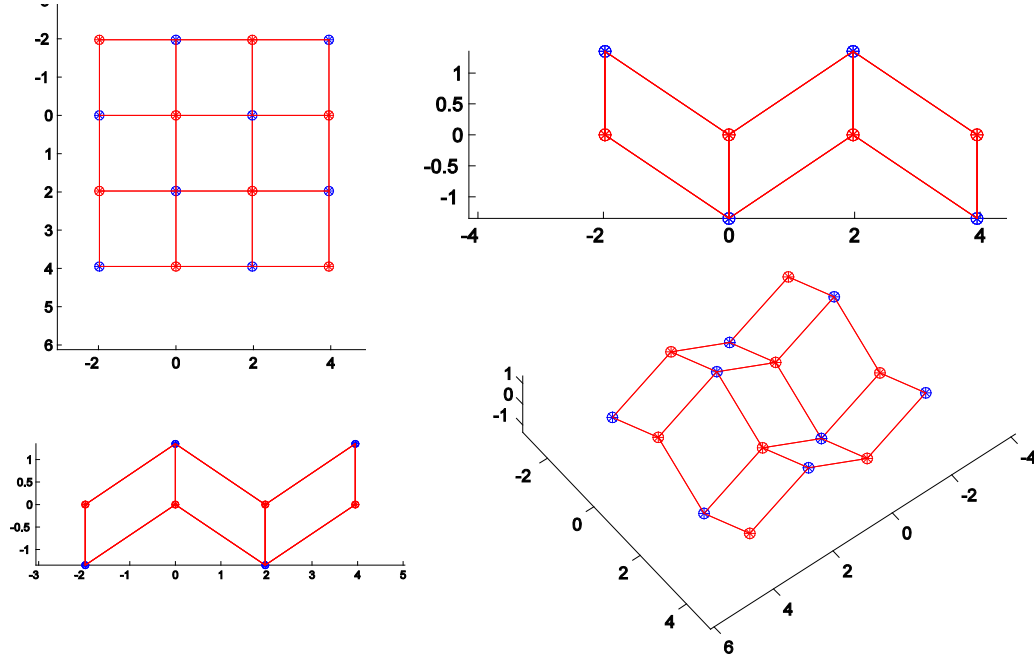


Figure 17. AIP with buckled square lattice is shown from different views (units in angstroms).

1.12 Bismuth Selenide

Bismuth selenide consists of three layers of Se and two layers of Bi (each unit cell of this material has five atoms). By performing structural relaxation, equilibrium lattice and basis vectors were calculated (in angstroms):

$$\mathbf{v}_1 = (0.866, \quad 0.50, \quad 0.00), \quad (\text{Equation 47})$$

$$\mathbf{v}_2 = (0.86, \quad -0.5, \quad 0.00), \quad (\text{Equation 48})$$

$$\mathbf{b}_1 = (4.78, \quad 0.00, \quad 8.10) \text{ atomic type: Se} \quad (\text{Equation 49})$$

$$\mathbf{b}_2 = (0.00, \quad 0.00, \quad 9.71) \text{ atomic type: Bi} \quad (\text{Equation 50})$$

$$\mathbf{b}_3 = (2.39, \quad 0.00, \quad 11.6) \text{ atomic type: Se} \quad (\text{Equation 51})$$

$$\mathbf{b}_4 = (4.78, \quad 0.00, \quad 13.6) \text{ atomic type: Bi} \quad (\text{Equation 52})$$

$$\mathbf{b}_5 = (0.00, \quad 0.00, \quad 15.2) \text{ atomic type: Se} \quad (\text{Equation 53})$$

The planar structure of this five-layer 2D material is shown in Figure 19.

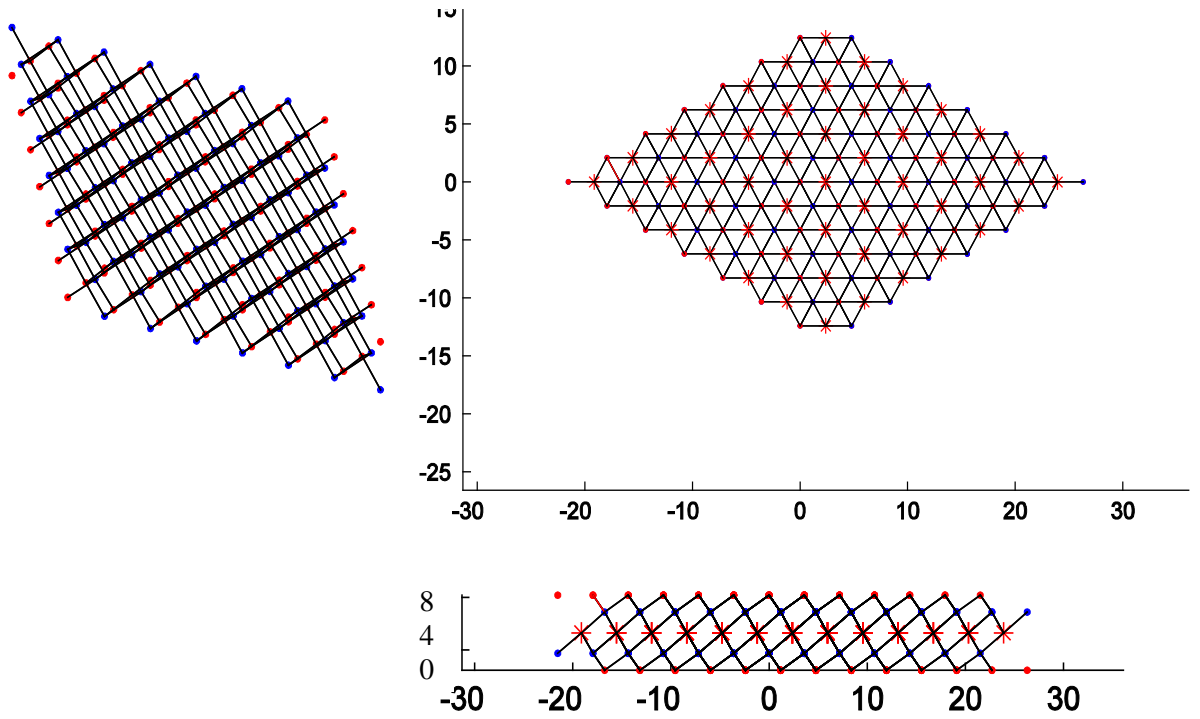


Figure 18. Bi_2Se_3 a 2D material with five atomic layers shown from three views (units in angstroms).

Deforming Bi_2Se_3 : The height of Gaussian bump was still 10 \AA and $\sigma = 15 \text{ \AA}$. The shape of the deformed patch is shown in Figure 19.

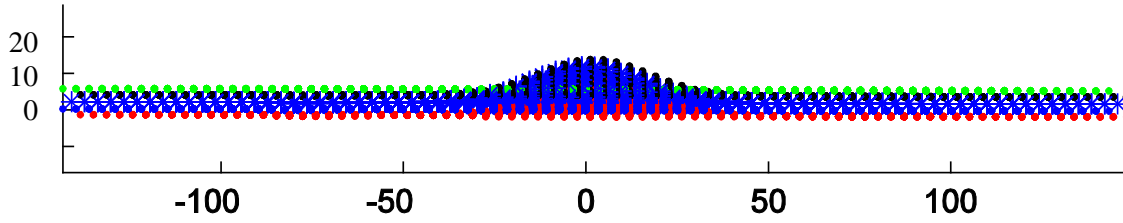


Figure 19. Gaussian deformation applied to Bi_2Se_3 . Different colors show different layers (units in angstroms).

Criteria of thickness reduction: The change in thickness of five layers computed using structural relaxation based on different lattice constants are presented in the Table 2. The relaxed thickness is also shown in bold.

Table 2. Thickness results from VASP for Bi_2Se_3

Lattice constant (Å)	3.94	3.99	4.04	4.09	4.14	4.19	4.29	4.34	4.39	4.49	4.54
Thickness (Å)	7.48	7.38	7.28	7.18	7.08	6.99	6.79	6.69	6.59	6.37	6.26

The thickness change in each layer are presented in Figure 20.

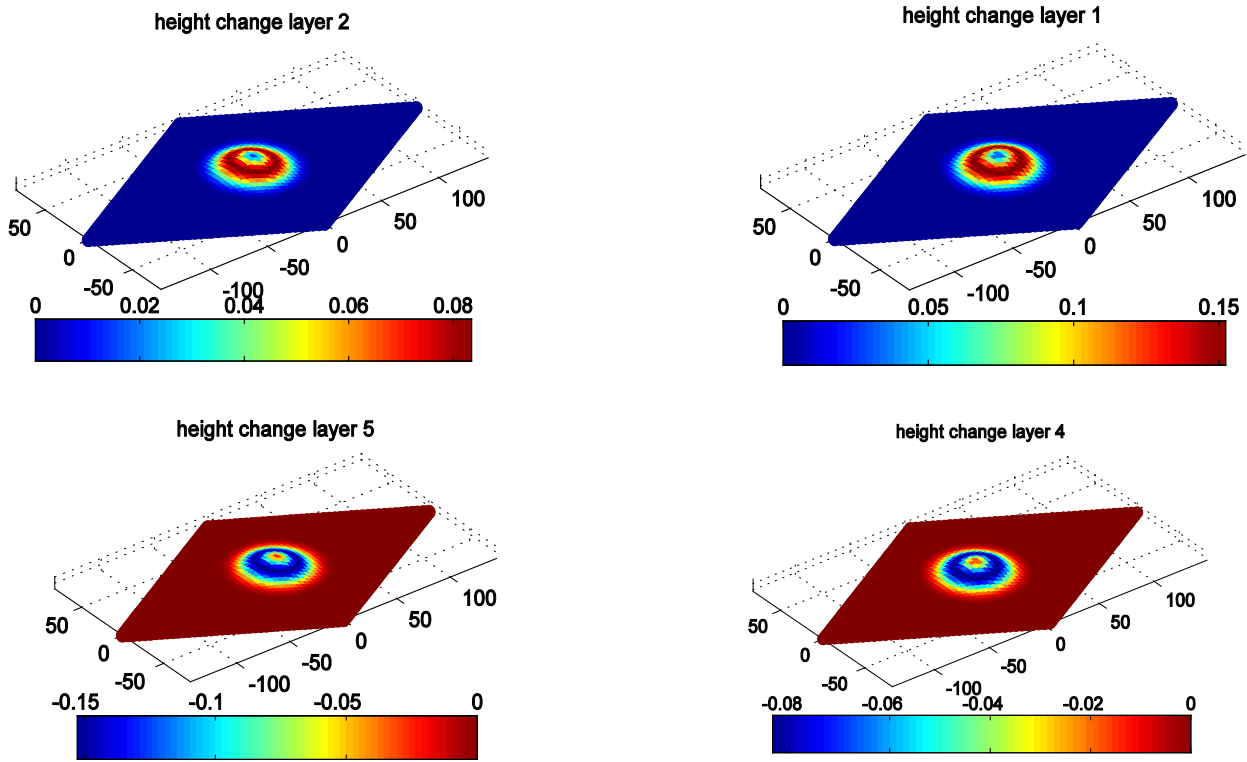


Figure 20. Optimum height reduction in a patch of Bi_2Se_3 in different layers (units in angstroms).

1.13 Lead

The structure of lead in a unit cell is also relaxed and lattice vector, basic vector, and lattice constant were computed (units in angstrom).

$$a_1 = 3.604 \text{ \AA}, \quad (\text{Equation 54})$$

$$\mathbf{v}_1 = (1.80, -3.12, 0.00), \quad (\text{Equation 55})$$

$$\mathbf{v}_2 = (1.80, 3.12, 0.00), \quad (\text{Equation 56})$$

$$\mathbf{b}_1 = (0.00, 0.00, 0.00), \quad (\text{Equation 57})$$

$$\mathbf{b}_2 = (1.80, 1.03, 2.74). \quad (\text{Equation 58})$$

Similar to other multilayer 2D materials, by exerting deformation to the structure of 2D lead, change in the thickness of the crystal was expected. This change in thickness was a function of lattice constant and is presented in Table 3.

Table 3. Thickness for Lead after an isotropic elongation.

Lattice constant (Å)	3.60	3.78	3.99	4.21	4.39	4.61	4.89	5.07	5.29
Thickness (Å)	2.52	2.40	2.29	2.20	1.97	1.67	1.65	1.64	1.63

The planar structure of Leadene is shown in Figure 21.

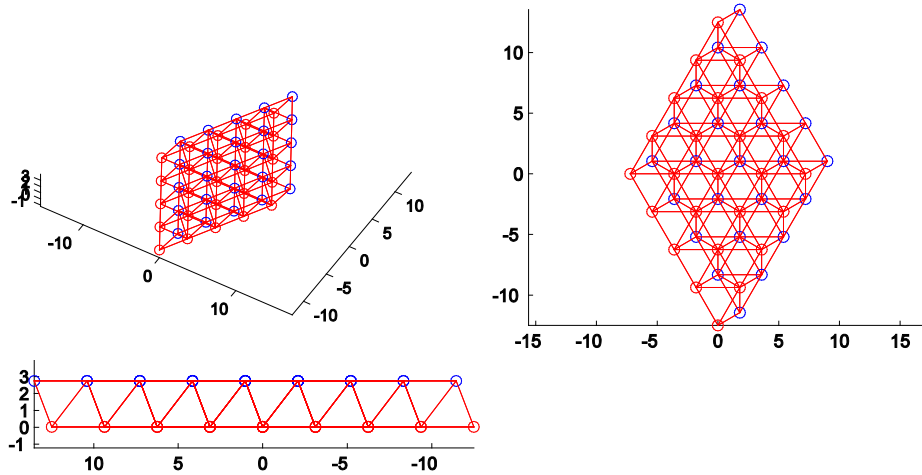


Figure 21. Leadene, a 2D material with two atomic layers, is shown from three views (units in angstroms).

1.14 Tungsten Diselenide

This 2D material has three layers which consists of two layers of selenium sandwiching a single layer of tungsten in the middle. By doing a structural relaxation, the optimal basis vectors were calculated. Each unit cell of this material has three atoms (units in angstroms).

$$\mathbf{v}_1 = (1.66, -2.87, 0.00), \quad (\text{Equation 59})$$

$$\mathbf{v}_2 = (1.66, 2.87, 0.00), \quad (\text{Equation 60})$$

$$\mathbf{b}_1 = (0.00, 0.00, 0.00), \quad (\text{Equation 61})$$

$$\mathbf{b}_2 = (1.66, 0.959, 1.70), \quad (\text{Equation 62})$$

$$\mathbf{b}_3 = (1.66, 0.959, -1.70). \quad (\text{Equation 63})$$

The planar structure of WSe₂ is shown in Figure 22:

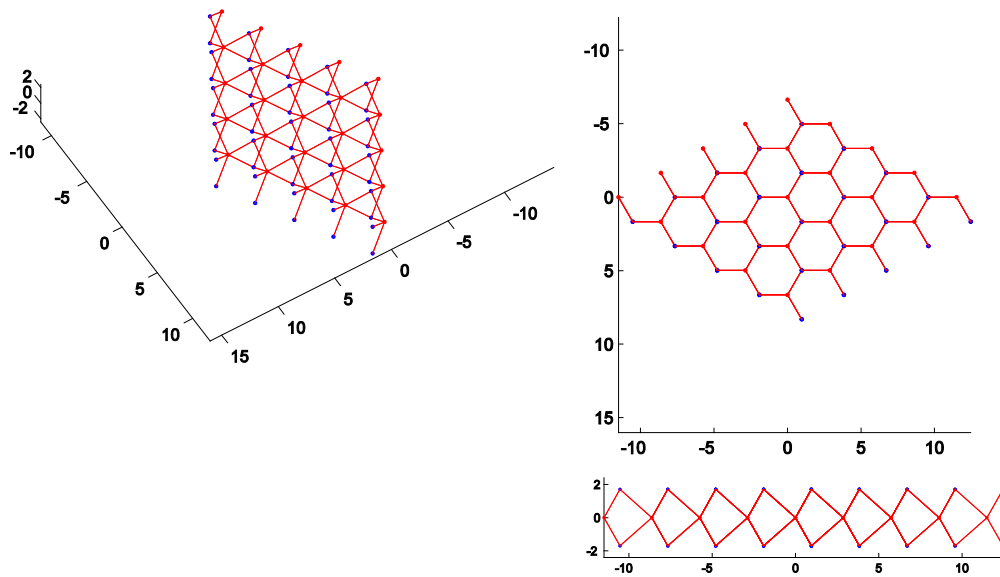


Figure 22. WSe₂, a 2D material with three atomic layers, is shown from three views (units in angstroms).

Thicknesses computed by structural relaxation based on different lattice constants are presented in Table 4; the optimum thickness is in bold.

Table 4. Thickness results from structural relaxation of WSe₂

Lattice constant (Å)	3.12	3.22	3.32	3.42	3.52	3.62	3.72	3.82	3.92
Thickness (Å)	3.56	3.48	3.40	3.33	3.26	3.20	3.15	3.10	3.04

1.15 Phosphorene

Phosphorus has many different allotropes with different colors. Red, blue, violet and white are some of these allotropes [35]. Among them, black phosphorus has captured researchers' interest recently [36-39]. In 1960, researchers proved that bulk black phosphorus has a high carrier mobility and band gap [40]. The band gap of bulk black phosphorus is about 0.31 to 0.36 eV. Similar to graphene which is exfoliated from graphite, one layer of black phosphorus can be mechanically exfoliated. The monolayer sheet is called phosphorene. Black phosphorus is the most stable allotrope of phosphorus [40]. Black phosphorus has a direct band gap ranging from 0.6 to 2 eV [37] depending upon the number of layers which makes it a potential material for high speed electronic devices. This property allures scientists to tune the band gap of black phosphorus by changing the number of the layers and use this material for different electronic and optic applications.

In addition to favorable band gap observed in multilayer black phosphorus, high mobility for holes, up to $1000 \text{ cm}^2\text{V}^{-1}\text{s}^{-1}$, has been observed.

Phosphorus is a very reactive material, especially in the air where it tends to react with oxygen. Therefore, researchers face a real challenge in using black phosphorus as an optical and electric material. However, many works have been reported in which field effect transistors are created by capping black phosphorus with a material called PMMA [37].

Black phosphorus structure:

Each unit cell consists of four atoms of phosphorus shown in Figure 23 with different colors. Equations 67-70 give the position of atoms in a cell (basis vectors). The two lattice

vectors of phosphorene after relaxation and also the lattice constants are shown by Equations 65 and 66 (units in angstroms).

$$a_1 = 3.30, \quad a_2 = 4.61, \quad (\text{Equation 64})$$

$$\mathbf{v}_1 = (3.30, \quad 0.00, \quad 0.00), \quad (\text{Equation 65})$$

$$\mathbf{v}_2 = (0.00, \quad 4.61, \quad 0.00), \quad (\text{Equation 66})$$

$$\mathbf{b}_1 = (-1.65, \quad -1.90, \quad -1.05), \quad (\text{Equation 67})$$

$$\mathbf{b}_2 = (0.00, \quad -0.415, \quad -1.05), \quad (\text{Equation 68})$$

$$\mathbf{b}_3 = (0.00, \quad 0.415, \quad 1.05), \quad (\text{Equation 69})$$

$$\mathbf{b}_4 = (1.65, \quad 1.90, \quad 1.05), \quad (\text{Equation 70})$$

In Table 5, the change in thickness of a black phosphorus 2D layer is shown against isotropic changes in lattice constants.

Table 5. Thickness for isotropic increase in lattice constant.

Lattice constant (Å)	3.25	3.26	3.27	3.29	3.30	3.32	3.35	3.55	3.75
Thickness (Å)	2.11	2.11	2.10	2.10	2.10	2.09	2.08	2.02	1.94

The lattice structure of black phosphorus is shown in Figure 23.

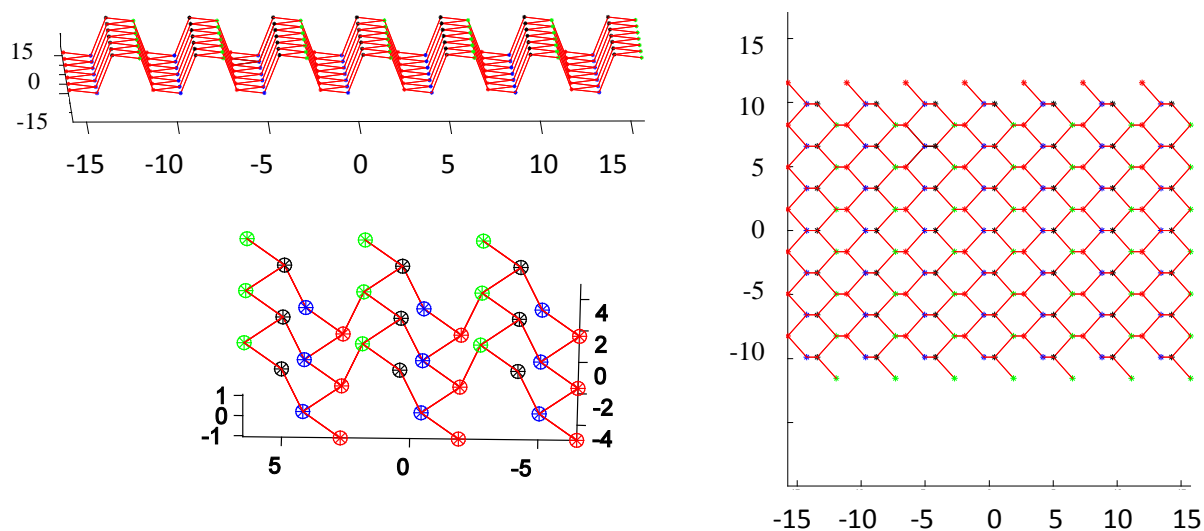


Figure 23. One layer of black phosphorus (phosphorene) from different views (units in angstroms).

Results and Discussion

1.16 Curvature Computation Results for Different Lattices

By following the various themes mentioned for different lattice structure, the local Gaussian and mean curvature of different 2D materials were computed.

Figures 24-28 show the Gaussian and mean curvature versus the distance to the center of the membrane. The curvature Figures show that since the deformation is identical for all materials, the curvature for all materials are identical regardless of their atomistic composition and shape, as expected for conformal deformations.

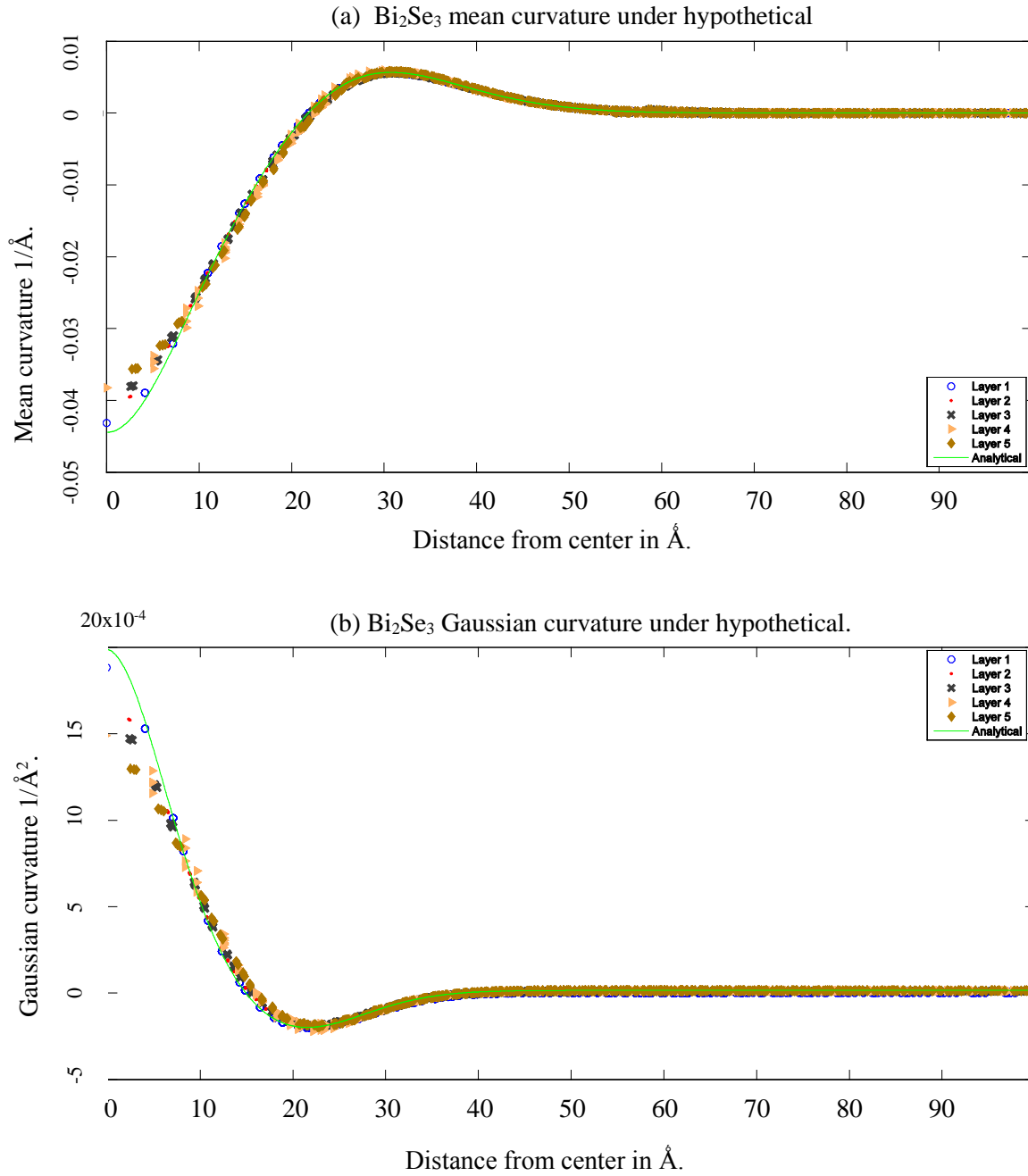


Figure 24. The Gaussian and mean curvature for Bi_2Se_3 . (a) Mean curvatures graphed vs. distance to the center; and, (b) the Gaussian curvature graphed vs. distance to the center. The solid line is an analytical prediction of the Gaussians and mean curvature.

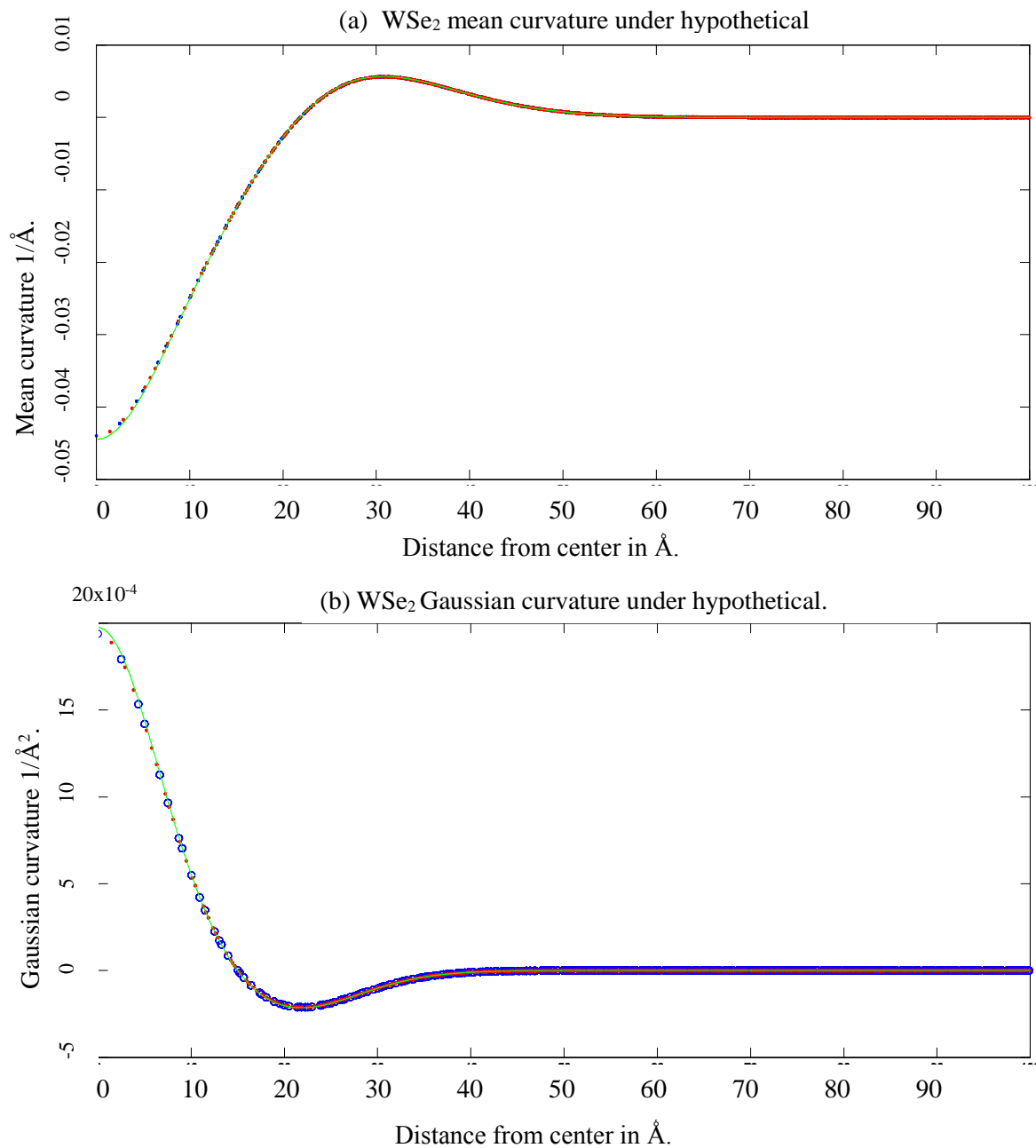


Figure 25. The Gaussian and mean curvature for WSe₂. (a) Mean curvatures graphed vs. distance to the center; and, (b) the Gaussian curvature graphed vs. distance to the center. The solid line is an analytical prediction of the Gaussians and mean curvature.

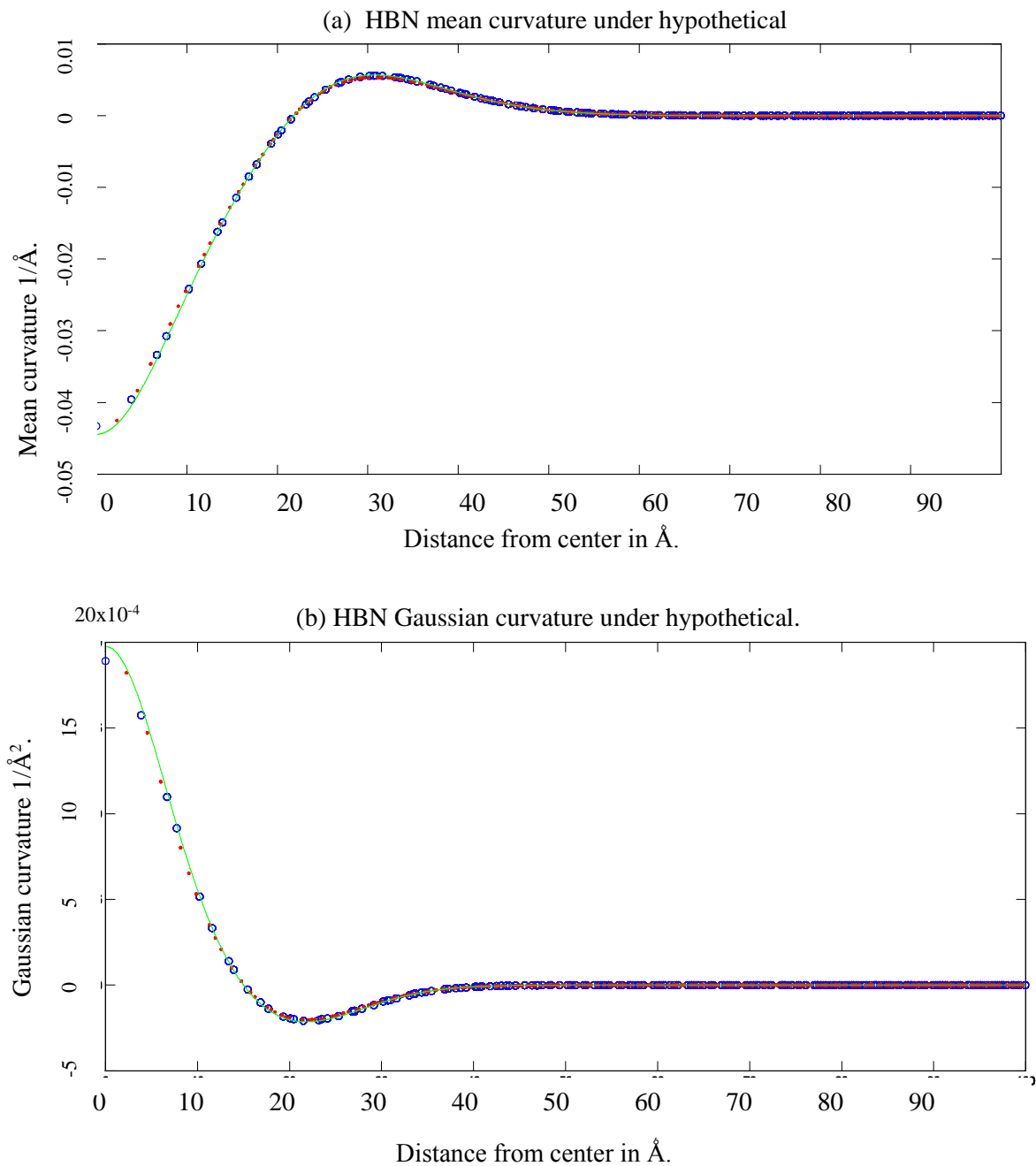


Figure 26. The Gaussian and mean curvature for HBN. (a) Mean curvatures graphed vs. distance to the center; and, (b) the Gaussian curvature graphed vs. distance to the center. The solid line is an analytical prediction of the Gaussians and mean curvature.

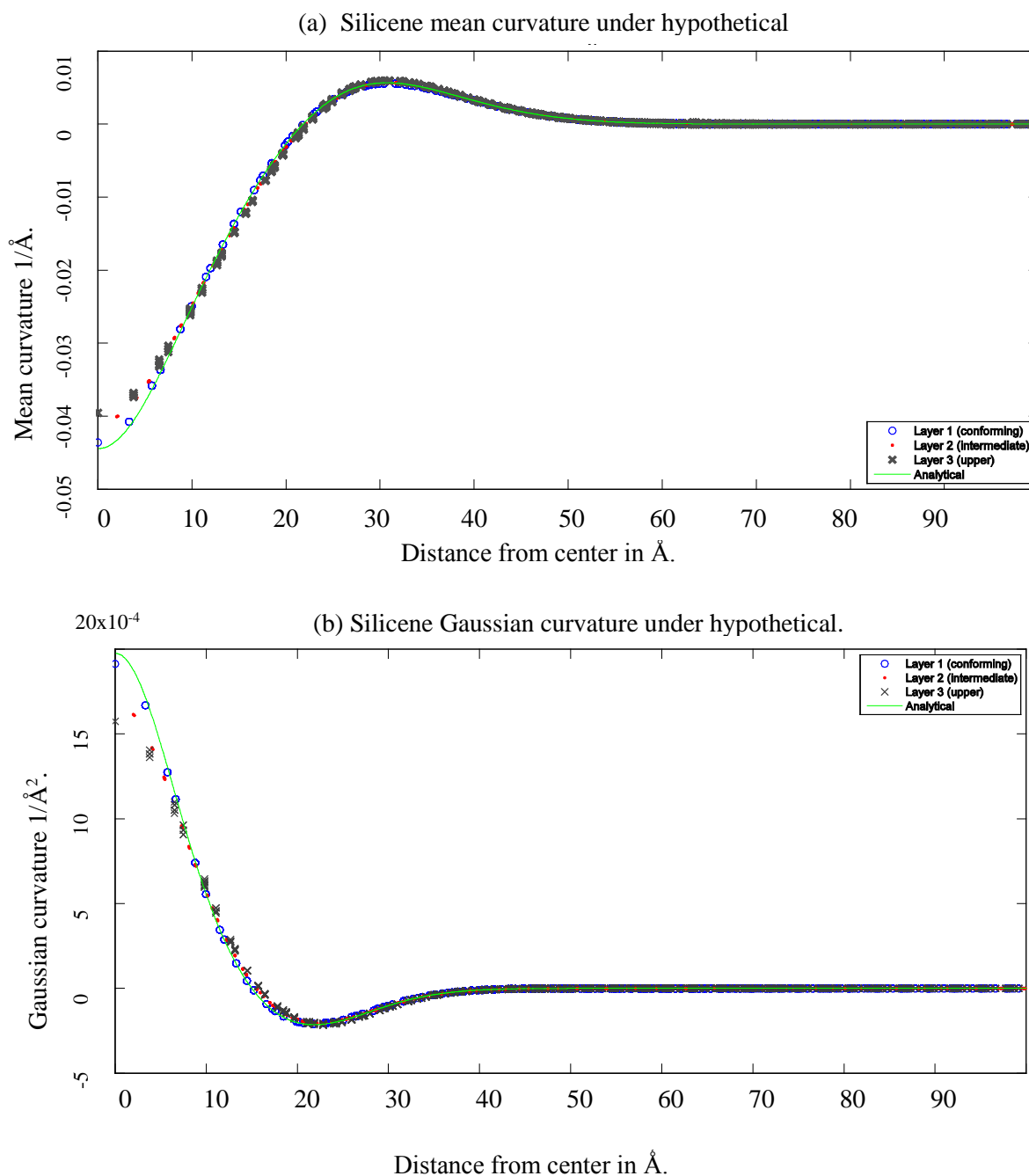


Figure 27. The Gaussian and mean curvature for silicene. (a) Mean curvatures graphed vs. distance to the center; and, (b) the Gaussian curvature graphed vs. distance to the center. The solid line is an analytical prediction of the Gaussians and mean curvature.

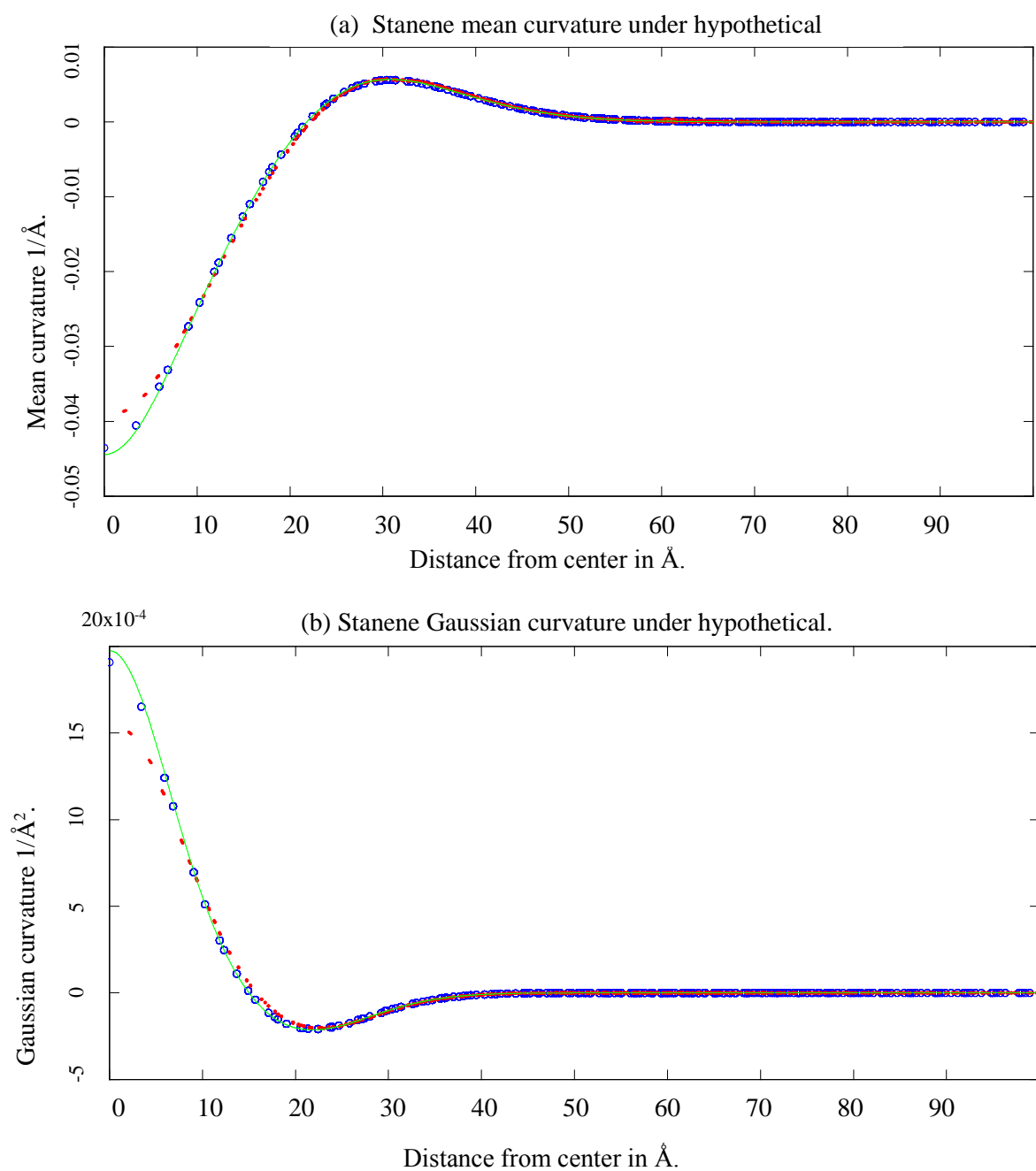


Figure 28. The Gaussian and mean curvature for high buckled stanene. (a) Mean curvatures graphed vs. distance to the center; and, (b) the Gaussian curvature graphed vs. distance to the center. The solid line is an analytical prediction of the Gaussians and mean curvature.

1.17 Metric Results for Various Lattices

The metric calculation for hexagonal boron nitride and bismuth selenide are presented here. The rest of structures had similar results and are not presented here.

Hexagonal BN

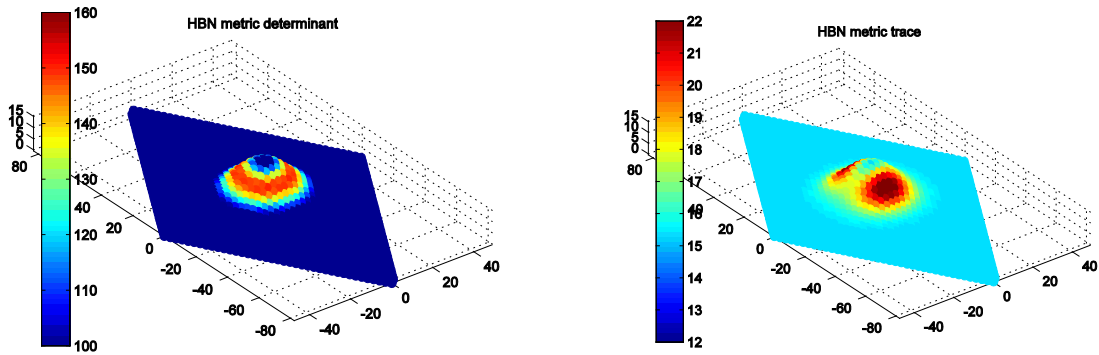


Figure 29. Left side: determinant of the metric tensor, right side: trace of metric tensor for hexagonal boron nitride (scales in Angstroms).

Bi_2Se_3

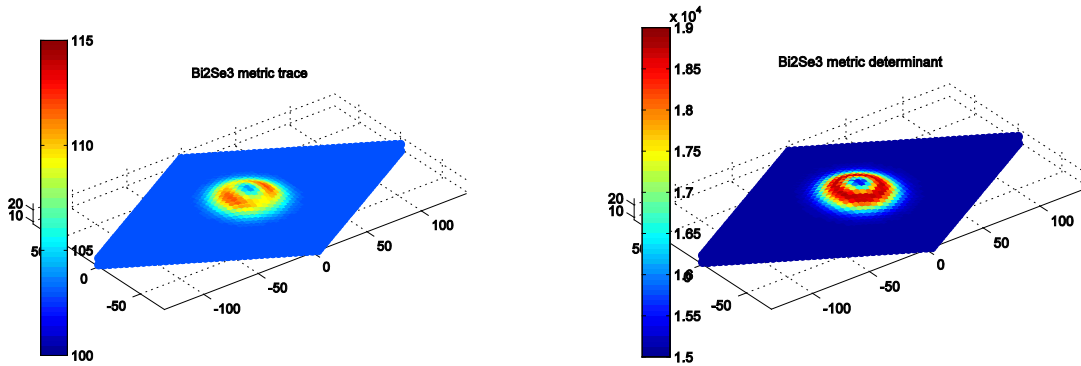


Figure 30. Left side: Determinant of the metric tensor, right side: trace of metric tensor for hexagonal Bi_2Se_3 (scales in Angstroms).

1.18 Conclusion:

Two-dimensional materials are materials with numerous unique properties. Compared to their bulk form, 2D materials have higher aspect ratio which makes them suitable for devices which need large surface to volume ratios. Another difference of 2D materials with their bulk form is the dependency of properties on their shapes. In literature, many researchers have tried to explore the geometry and the effect of shape on chemical and electronic properties of 2D materials by applying known thin plate theories [41-46]. However, these theories are only applicable for large patch of atoms and under small deformation regimes. In most cases, the deformation of 2D materials is significantly large and the properties can be changed (and consequently tuned) when the deformation is more than 20 percent. In these circumstances, the use of continuum theories to investigate the shape of 2D materials is questionable.

In this research, a discrete method was presented to investigate the local geometry of 2D materials without relying on continuum approximation and thin plate theory. In fact, the discrete nature of 2D materials especially in nano-structures require researchers to rely on discrete methods rather than fitting continuum surfaces to deformed membranes. The four invariants of geometry of 2D materials were calculated. The results show that the calculation of discrete curvature using the method presented in this research agree very well with analytical results for both the Gaussian and mean curvature when the structure of materials are changed. The method was also generalized for structural defects, for example, when pentagon and heptagon were inserted in the structure of a hexagonal lattice.

The Gaussian and mean calculation using this method was stable as six or more than six vertices were used to calculate the curvatures. However, there are some methods to extract

curvature even for five vertices. These methods may be helpful for unknown structures that have only five nearest neighbors.

The metric tensor was also computed using the dot product of lattice vectors (metric tensor which shows how much the membrane is stretched compared to pre-deformed membrane). However, further research on the metric is needed when the membrane goes to the third dimension as in Bi_2Se_3 and black phosphorus.

References:

- [1] M. I. Katsnelson, "Graphene: carbon in two dimensions," *Materials Today*, vol. 10, pp. 20-27, 2007.
- [2] V. M. Pereira and A. C. Neto, "Strain engineering of graphene's electronic structure," *Phys. Rev. Lett.*, vol. 103, pp. 046801, 2009.
- [3] A. A. Pacheco Sanjuan, M. Mehboudi, E. O. Harriss, H. Terrones and S. Barraza-Lopez, "Quantitative Chemistry and the Discrete Geometry of Conformal Atom-Thin Crystals," *ACS Nano*, vol. 8, pp. 1136-1146, 2014.
- [4] A. A. P. Sanjuan, Z. Wang, H. P. Imani, M. Vanević and S. Barraza-Lopez, "Graphene's morphology and electronic properties from discrete differential geometry," *Physical Review B*, vol. 89, pp. 121403, 2014.
- [5] K. Novoselov, A. K. Geim, S. Morozov, D. Jiang, M. K. I. Grigorieva, S. Dubonos and A. Firsov, "Two-dimensional gas of massless Dirac fermions in graphene," *Nature*, vol. 438, pp. 197-200, 2005.
- [6] D. R. Dreyer, R. S. Ruoff and C. W. Bielawski, "From conception to realization: An historical account of graphene and some perspectives for its future," *Angewandte Chemie International Edition*, vol. 49, pp. 9336-9344, 2010.
- [7] H. Boehm and E. Stumpp, "Citation errors concerning the first report on exfoliated graphite," *Carbon*, vol. 45, pp. 1381-1383, 2007.
- [8] C. Schafhaeuti, "LXXXVI. On the combinations of carbon with silicon and iron, and other metals, forming the different species of cast iron, steel, and malleable iron," *The London and Edinburgh Philosophical Magazine and Journal of Science*, vol. 16, pp. 570-590, 1840.
- [9] Ş. ŢiŢeica, "Über die Widerstandsänderung von Metallen im Magnetfeld," *Annalen Der Physik*, vol. 414, pp. 129-161, 1935.
- [10] N. D. Mermin, "Crystalline order in two dimensions," *Physical Review*, vol. 176, pp. 250, 1968.
- [11] H. Boehm, R. Setton and E. Stumpp, "Nomenclature and terminology of graphite intercalation compounds," *Carbon*, vol. 24, pp. 241-245, 1986.
- [12] K. S. Novoselov, D. Jiang, F. Schedin, T. J. Booth, V. V. Khotkevich, S. V. Morozov and A. K. Geim, "Two-dimensional atomic crystals," *Proc. Natl. Acad. Sci. U. S. A.*, vol. 102, pp. 10451-10453, Jul 26, 2005.

- [13] F. Halzen and A. D. Martin, "Quarks and leptons: An introductory course in modern particle physics," 1996.
- [14] K. K. Gomes, W. Mar, W. Ko, F. Guinea and H. C. Manoharan, "Designer Dirac fermions and topological phases in molecular graphene," *Nature*, vol. 483, pp. 306-310, 2012.
- [15] R. Lieth, *Preparation and Crystal Growth of Materials with Layered Structures*. Springer, 1977.
- [16] E. Rokuta, Y. Hasegawa, K. Suzuki, Y. Gamou, C. Oshima and A. Nagashima, "Phonon dispersion of an epitaxial monolayer film of hexagonal boron nitride on Ni (111)," *Phys. Rev. Lett.*, vol. 79, pp. 4609, 1997.
- [17] H. Liu, A. T. Neal, Z. Zhu, D. Tomanek and P. D. Ye, "Phosphorene: A New 2D Material with High Carrier Mobility," *arXiv Preprint arXiv:1401.4133*, 2014.
- [18] B. Radisavljevic, A. Radenovic, J. Brivio, V. Giacometti and A. Kis, "Single-layer MoS2 transistors," *Nature Nanotechnology*, vol. 6, pp. 147-150, 2011.
- [19] X. Huang, Z. Yin, S. Wu, X. Qi, Q. He, Q. Zhang, Q. Yan, F. Boey and H. Zhang, "Graphene-Based Materials: Synthesis, Characterization, Properties, and Applications," *Small*, vol. 7, pp. 1876-1902, 2011.
- [20] R. Mas-Balleste, C. Gomez-Navarro, J. Gomez-Herrero and F. Zamora, "2D materials: to graphene and beyond," *Nanoscale*, vol. 3, pp. 20-30, 2011.
- [21] L. Xian, S. Barraza-Lopez and M. Chou, "Effects of electrostatic fields and charge doping on the linear bands in twisted graphene bilayers," *Physical Review B*, vol. 84, pp. 075425, 2011.
- [22] N. Mohanty and V. Berry, "Graphene-based single-bacterium resolution biodevice and DNA transistor: interfacing graphene derivatives with nanoscale and microscale biocomponents," *Nano Letters*, vol. 8, pp. 4469-4476, 2008.
- [23] F. de Juan, J. L. Mañes and M. A. Vozmediano, "Gauge fields from strain in graphene," *Physical Review B*, vol. 87, pp. 165131, 2013.
- [24] C. Lee, X. Wei, J. W. Kysar and J. Hone, "Measurement of the elastic properties and intrinsic strength of monolayer graphene," *Science*, vol. 321, pp. 385-388, Jul 18, 2008.
- [25] F. Guinea, "Strain engineering in graphene," *Solid State Commun.*, vol. 152, pp. 1437-1441, 2012.
- [26] M. A. Vozmediano, M. Katsnelson and F. Guinea, "Gauge fields in graphene," *Physics Reports*, vol. 496, pp. 109-148, 2010.

- [27] J. V. Sloan, A. A. P. Sanjuan, Z. Wang, C. Horvath and S. Barraza-Lopez, "Strain gauge fields for rippled graphene membranes under central mechanical load: An approach beyond first-order continuum elasticity," *Physical Review B*, vol. 87, pp. 155436, 2013.
- [28] A. I. Bobenko, J. M. Sullivan and P. Schr, *Discrete Differential Geometry*. Springer, 2008.
- [29] W. Kühnel, *Differential Geometry: Curves-Surfaces-Manifolds*. American Mathematical Soc., 2006.
- [30] S. Alexander, P. Chaikin, P. Grant, G. Morales, P. Pincus and D. Hone, "Charge renormalization, osmotic pressure, and bulk modulus of colloidal crystals: Theory," *J. Chem. Phys.*, vol. 80, pp. 5776-5781, 1984.
- [31] H. T. Grahn, *Introduction to Semiconductor Physics*. World Scientific, 1999.
- [32] Z. Xu and G. Xu, "Discrete schemes for Gaussian curvature and their convergence," *Comput. Math. Appl.*, vol. 57, pp. 1187-1195, 2009.
- [33] V. Borrelli, F. Cazals and J. Morvan, "On the angular defect of triangulations and the pointwise approximation of curvatures," *Comput. Aided Geom. Des.*, vol. 20, pp. 319-341, 2003.
- [34] U. Pinkall and K. Polthier, "Computing discrete minimal surfaces and their conjugates," *Experimental Mathematics*, vol. 2, pp. 15-36, 1993.
- [35] N. N. Greenwood and A. Earnshaw, *Chemistry of the Elements*. Elsevier, 1997.
- [36] M. Engel, M. Steiner and P. Avouris, "A black phosphorus photo-detector for multispectral, high-resolution imaging," *arXiv Preprint arXiv:1407.2534*, 2014.
- [37] L. Li, Y. Yu, G. J. Ye, Q. Ge, X. Ou, H. Wu, D. Feng, X. H. Chen and Y. Zhang, "Black phosphorus field-effect transistors," *Nature Nanotechnology*, 2014.
- [38] F. Xia, H. Wang and Y. Jia, "Rediscovering Black Phosphorus: A Unique Anisotropic 2D Material for Optoelectronics and Electronics," *arXiv Preprint arXiv:1402.0270*, 2014.
- [39] Z. Zhu and D. Tománek, "Semiconducting layered blue phosphorus: A computational study," *Phys. Rev. Lett.*, vol. 112, pp. 176802, 2014.
- [40] H. Liu, A. T. Neal, Z. Zhu, Z. Luo, X. Xu, D. Tománek and P. D. Ye, "Phosphorene: An Unexplored 2D Semiconductor with a High Hole Mobility," *ACS Nano*, vol. 8, pp. 4033-4041, 2014.
- [41] S. Pradhan and T. Murmu, "Small scale effect on the buckling analysis of single-layered graphene sheet embedded in an elastic medium based on nonlocal plate theory," *Physica E: Low-Dimensional Systems and Nanostructures*, vol. 42, pp. 1293-1301, 2010.

- [42] J. Atalaya, A. Isacsson and J. M. Kinaret, "Continuum elastic modeling of graphene resonators," *Nano Letters*, vol. 8, pp. 4196-4200, 2008.
- [43] Q. Lu, M. Arroyo and R. Huang, "Elastic bending modulus of monolayer graphene," *J. Phys. D*, vol. 42, pp. 102002, 2009.
- [44] S. Pradhan and J. Phadikar, "Small scale effect on vibration of embedded multilayered graphene sheets based on nonlocal continuum models," *Physics Letters A*, vol. 373, pp. 1062-1069, 2009.
- [45] L. Shen, H. Shen and C. Zhang, "Nonlocal plate model for nonlinear vibration of single layer graphene sheets in thermal environments," *Computational Materials Science*, vol. 48, pp. 680-685, 2010.
- [46] C. Wang, K. Mylvaganam and L. Zhang, "Wrinkling of monolayer graphene: a study by molecular dynamics and continuum plate theory," *Physical Review B*, vol. 80, pp. 155445, 2009.

Appendix A: Description of Research for Popular Publication

Title: Characterizing shape of 2D materials.

A new framework is developed to characterize the shape of graphene and other 2D materials in Dr. Barraza Lopez research group. Mehrshad Mehboudi is a Micro E-P student and a member of this group who has contributed to these developments.

2D materials are a class of materials that are very thin and their width and length are huge compared to their thickness. Most of these materials have only one to few atoms in thickness. For a long time scientists believed that these 2D materials are not stable in the environment, however in 2004 two scientists synthesized one of the first 2D materials made of carbon (Later on they won physics nobel prize for their discovery). Very soon numerous types of 2D materials made of different elements were synthesized. There is a fact about these materials that has made researchers hopeful to make new devices using these materials. The properties these materials are extremely dependent on their shape. That means if someone stretch a patch of graphene its ability to conduct electricity, would change. Therefore all researchers know that the shape of 2D materials are important and they should conduct more research on this subject. In this master thesis we implement a branch of geometry called discrete differential geometry to discuss the important parameter using which we can discuss the shape of 2D material.

There are four parameters in discrete geometry that are important in telling the shape of a 2D material. Two parameters come from curvature which shows how much the material is bended. And two parameters come from metric which show how much the material is stretched in different directions. In this thesis we calculated the mentioned shape parameters and compared it

with some known values for known mathematical function and realized that the method is quite accurate and useful.

Appendix B: Executive Summary of Newly Created Intellectual Property

The intellectual property created in this research:

- 1- The estimation of discrete curvature and metric to 2D structures such as single atom layer crystals, two layer buckled crystals, and multi-layer 2D materials.
- 2- Several MATLAB codes for calculating curvature, metric and building structures.

Appendix C: Potential Patent and Commercialization Aspects of listed Intellectual Property Items

C.1 Patentability of Intellectual Property (Could Each Item be Patented)

1- Not Patentable.

C.2 Commercialization Prospects (Should Each Item Be Patented)

The discrete geometry framework could not be patented as a commercialized product.
The code also cannot be patented as a commercialized product.

C.3 Possible Prior Disclosure of IP

The local geometry framework is being published so it is disclosed to the public. The MATLAB codes are not disclosed to the public and it is only available in the research group. The code can be shared if direct interest arises.

Appendix D: Broader Impact of Research

D.1 Applicability of Research Methods to Other Problems

The discrete method to discuss the geometry of 2D materials can be applied to all 2D crystals to discuss the local shape of these crystals. The method also can be used in any research that relates the local geometry to the properties of 2D materials.

D.2 Impact of Research Results on U.S. and Global Society

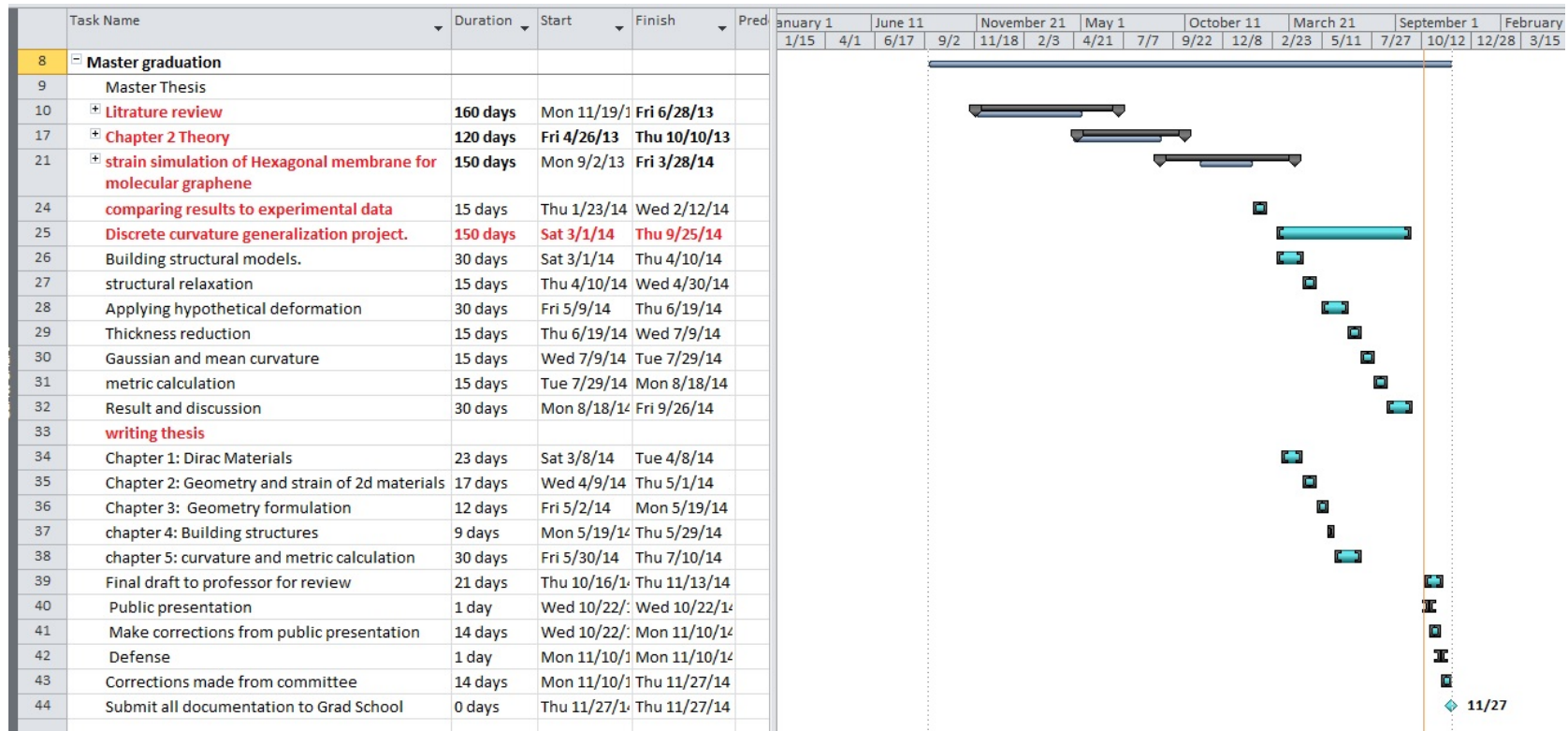
The method could be used to discuss the shape of 2D crystals accurately compared to current continuum methods, and down the road will be useful to correlate the properties of 2D crystals to their shape.

D.3 Impact of Research Results on the Environment.

Not foreseeable.

Appendix E: Microsoft Project for MS MicroEP Degree Plan.

59



Appendix F: Identification of All Software Used in Research and Thesis Generation

Computer #1:

Model Number: Dell Dimension 8300

Serial Number:

Location: Kimpel 240

Owner: Dr. Barraza Lopez

Software #1:

Name: Apache open-office

Free License: Downloaded by Mehrshad Mehboudi

Software #2:

Name: MATLAB 2013

Purchased by: Salvador Barraza Lopez

Software #3:

Name: Adobe Acrobat Professional 10.0

Purchased by: UA

Software #4

Name: Jmol

Free License: Downloaded by Mehrshad Mehboudi

Software #4:

Name: VMD

Free License: Downloaded by Mehrshad Mehboudi

Computer #2:

Model Number: Dell

Serial Number:

Location: Kimpel 240

Owner: Dr. Barraza Lopez

Software #1:

Name: Linux Ubuntu

Free License: Downloaded by Mehrshad Mehboudi

Software #2: VASP

Name: Apache open-office

Free License: Downloaded Salvador Barraza-Lopez

Computer #2: Mullin library computers

Software #1:

Name: Matlab 2013

Purchased by: UA

Software #2:

Name: Microsoft Office

Purchased by: UA

Software #3:

Name: Adobe Acrobat readers

Purchased by: UA

Appendix G: All Publications Published, Submitted and Planned

- 1- Pacheco Sanjuan, A. A., Mehboudi, M., Harriss, E. O., Terrones, H., & Barraza-Lopez, S. “Quantitative Chemistry and the Discrete Geometry of Conformal Atom-Thin Crystals. ACS nano,” 8(2), 1136-1146. (2014).
- 2- Mehboudi, M., Utt, K., Terrones, H., Pacheco, A., Harriss, E., & Barraza-Lopez, S. “Atom-based geometrical fingerprinting of conformal two-dimensional materials”. Physical Letter Review. To be submitted in December, 2014.